Applied Water Science (2023) 13:20
https://doi.org/10.1007/s13201-022-01827-9

REVIEW ARTICLE

Adsorption mechanism and modeling of radionuclides and heavy metals onto ZnO nanoparticles: a review

Kovo G. Akpomie[1,2] · Jeanet Conradie[2] · Kayode A. Adegoke[3] · Kabir O. Oyedotun[4] · Joshua. O. Ighalo[5,6] · James F. Amaku[7] · Chijioke Olisah[8] · Adedapo O. Adeola[3,9] · Kingsley O. Iwuozor[10]

Received: 19 August 2022 / Accepted: 10 November 2022 / Published online: 27 November 2022
© The Author(s) 2022

Abstract

The contamination of environmental waters with heavy metals and radionuclides is increasing because of rapid industrial and population growth. The removal of these contaminants from water via adsorption onto metal nanoparticles is an efficient and promising technique to abate the toxic effects associated with these pollutants. Among metal nanoparticle adsorbents, zinc oxide nanoparticles (ZnONPs) have received tremendous attention owing to their biocompatibility, affordability, long-term stability, surface characteristics, nontoxicity, and powerful antibacterial activity against microbes found in water. In this review, we considered the adsorption of heavy metals and radionuclides onto ZnONPs. We examined the isotherm, kinetic, and thermodynamic modeling of the process as well as the adsorption mechanism to provide significant insights into the interactions between the pollutants and the nanoparticles. The ZnONPs with surface areas (3.93 to 58.0 m^2/g) synthesized by different methods exhibited different adsorption capacities (0.30 to 1500 mg/g) for the pollutants. The Langmuir and Freundlich isotherms were most suitable for the adsorption process. The Langmuir separation factor indicated favorable adsorption of all the pollutants on ZnONPs. The pseudo-second-order kinetics presented the best for the adsorption of the adsorbates with regression values in the range of 0.986–1.000. Spontaneous adsorption was obtained in most of the studies involving endothermic and exothermic processes. The complexation, precipitation, ion exchange, and electrostatic interactions are the probable mechanisms in the adsorption onto ZnONPs with a predominance of complexation. The desorption process, reusability of ZnONPs as well as direction for future investigations were also presented.

Keyword Adsorption mechanism · Adsorbent reusability · Environment · Wastewater treatment · ZnO nanoparticles

Abbreviations

A	Equilibrium binding energy (L/mg)
ATR-FTIR	Attenuated total reflection-Fourier transform infrared
B	Temkin's constant (mg/g)
β	Dubinin–Radushkevich energy constant (mol^2/J^2)
C	Intercept of intraparticle diffusion
C_e	Equilibrium concentration (mg/L)
$\Delta G°$	Standard Gibbs free energy change (kJ/mol)

✉ Kovo G. Akpomie
kovo.akpomie@unn.edu.ng

[1] Department of Pure and Industrial Chemistry, University of Nigeria, Nsukka, Nigeria

[2] Department of Chemistry, University of the Free State, Bloemfontein 9300, South Africa

[3] Department of Chemical Sciences, University of Johannesburg, Doornfontein 2028, South Africa

[4] College of Science, Engineering and Technology (CSET), University of South Africa, Florida Campus, Johannesburg 1710, South Africa

[5] Department of Chemical Engineering, Nnamdi Azikiwe University, P.M.B. 5025, Awka, Nigeria

[6] Department of Chemical Engineering, Kansas State University, Manhattan, KS, USA

[7] Department of Chemistry, Michael Okpara University of Agriculture, Umudike, Nigeria

[8] Department of Botany, Institute for Coastal and Marine Research (CMR), Nelson Mandela University, Port Elizabeth, South Africa

[9] Department of Chemical Sciences, Adekunle Ajasin University, Akungba-Akoko, Ondo State, Nigeria

[10] Department of Pure and Industrial Chemistry, Nnamdi Azikiwe University, Awka, Nigeria

ΔH°	Standard enthalpy change (kJ/mol)
ΔS°	Standard entropy change (J/mol K)
ε	Polanyi potential
FTIR	Fourier transform infrared
K_1	Pseudo-first-order rate constant (min^{-1})
K_2	Pseudo-second-order rate constant (g/mg min)
K_d	Intraparticle diffusion rate constant (mg/g $min^{1/2}$)
K_F	Freundlich adsorption capacity (mg/g)
K_L	Langmuir adsorption constant (L/mg)
n	Freundlich adsorption intensity
q_e	Adsorption capacity (mg/g)
q_L	Maximum monolayer adsorption capacity (mg/g)
q_m	Theoretical saturation capacity (mg/g)
q_t	Adsorption capacity at a given time (mg/g)
R^2	Coefficient of determination
R_L	Separation factor
SEM	Scanning electron microscopy
t	Adsorption time (min)
USEPA	United States Environmental Protection Agency
XPS	X-ray photoelectron spectroscopy
XRD	X-ray diffraction
ZnONPs	Zinc oxide nanoparticles

Introduction

Clean water is needed all over the world for the health and well-being of living things (Tortajada and Biswas 2018). Clean water scarcity has become a serious problem in most developing, as well as some developed countries (Falkenmark 2022). This is due to rapid technological growth, industrial effluent pollution, a fast increase in human population, and irregular rainfall, affecting water quality (Bello et al. 2018). Regular use of modern facilities and products in our day-to-day activities, such as petrol in cars, plastics, textile clothing, food products, and drugs, just to mention a few, have generated large amounts of waste products, which have significantly contaminated pristine water bodies (Ahmad and Danish 2018; Ogbu et al. 2019). The use of polluted waters has resulted in severe adverse effects on plants, humans, and living organisms in general (Ezemonye et al. 2019; Lellis et al. 2019). Groundwater which is the most reliable source of clean water for use by the local population in developing countries is rapidly being polluted from the agricultural application of pesticides and fertilizers, as well as from organic and inorganic effluent discharge from industries (Edokpayi et al. 2018; Kiwaan et al. 2020; Asiwaju-Bello et al. 2020). In recent years, toxic pollutants were found to be present in unacceptable quantities in water in some developing countries, which poses a serious health threat to the local population (Ahmad and Danish 2018; Imran et al. 2020). Previously, when pollutant discharge to the environment was still low, contaminated waters were easily remediated by the adsorption process of soil, allowing clean water to penetrate, filter through, and get accumulated in underground water sources. Recently, due to the sharp increase in the release and concentration of pollutants, the soil uptake capacities have become saturated, thus also allowing the penetration of pollutants to underground sources.

Heavy metals are one of the most dangerous contaminants damaging the environment (Vardhan et al. 2019). Metals are natural elements that have been mined from the soil and used for human industry and products for millennia, making them a prominent source of worldwide distributed pollution. The massive growth in heavy metals use over the last few decades has undoubtedly resulted in an increase in metallic substance flux in the aquatic and terrestrial environment (Gautam et al. 2016). Due to their toxicity, longevity in the environment, non-biodegradability, and accumulation in the food chain, heavy metal contamination in aqueous media and industrial effluents is a serious ecological hazard (Chukwuemeka-Okorie et al. 2018; Mitra et al. 2022). At certain amounts, most heavy metals are carcinogenic. Zinc, copper, nickel, mercury, cadmium, lead, cobalt, arsenic, and chromium are toxic heavy metals of particular concern in the environment (Uddin 2017; Chakraborty et al. 2022). Similarly, the rising usage of radioactive materials in nuclear power plants, nuclear medicine, research, industry, and agriculture has raised the likelihood of radioactive water pollution (Yu et al. 2015). There have been various nuclear incidents in the past that have resulted in direct radioactive poisoning of water. These include the Fukushima Daiichi nuclear power plant accident in Japan in 2011, the Chernobyl disaster in Russia in 1986, the Three Mile Island nuclear power plant accident in the United States in 1979, the Kyshtym nuclear power plant explosion in Russia in 1975, and the K-19 nuclear power plant explosion in the North Atlantic in 1961 (Wang and Zhuang 2019; Kumar et al. 2020). The pollution of environmental waters with radionuclides such as uranium, thorium, selenium, lanthanum, cerium, ruthenium, and vanadium can also be associated with some toxic effects at a certain concentration (Gendy et al. 2021; Hassan et al. 2022; Akl 2022; Niu et al. 2022; Ji and Zhang 2022). The sources, harmful effects, and the United States Environmental Protection Agency's (USEPA) permissible limits of heavy metals and radionuclides in drinking water are presented in Table 1.

As a result of the hazardous effects associated with heavy metal and radionuclide pollution of environmental waters, numerous strategies for treating contaminated waters have been developed. Electrochemical treatment, forward osmosis, flotation, reverse osmosis, lime softening, ion exchange, filtration, adsorption, solvent extraction, electrodialysis,

Table 1 The US Environmental Protection Agency's maximum permissible limit, sources, and toxicity of heavy metals and radionuclides

Element	USEPA (mg/L)	Source	Harmful effect	References
Copper	1.300	Industrial emissions, Smelting, electroplating, sludge, pesticides, plastic industries, etching, cardboard processing, pigments, petroleum refining, pickling tanks, and mining industries	Eyes, mouth, and nose irritations, stomach problems, headaches, carcinogenic, heart disease, osteoporosis, fatigue, seizures, insomnia, and mental disorders	(Gautam et al. 2016; Uddin 2017; Afroze and Sen 2018; Saadat et al. 2020; Khan et al. 2021; Gao et al. 2022)
Chromium	0.100	Leather tanning, textile industries, salts manufacturing, industrial coolants, mining, petroleum refining, pulp processing, electroplating, ceramics, fertilizer industries, and chrome plating	Liver and kidney damage, carcinogenic, eye and skin irritation, ulcerations, teratogenic, mutagenic, allergic dermatitis, tumors, diarrhea, and vomiting	(Yang et al. 2015; Gautam et al. 2016; Uddin 2017; Eliodorio et al. 2017; Afroze and Sen 2018; Amaku et al. 2021, 2022)
Uranium	0.030	Nuclear power plants, uranium mill tailings, ammunition shave, and metallurgical industries	Kidney damage, retards normal metabolism, skin erythema, leukemia, nephritis, trichomadesis, genetic mutations, physical lesions, chronic poisoning, and bone cancer	(Bird 2012; Xiao-teng et al. 2019; Wu et al. 2019; Akl 2022; Su et al. 2022)
Lead	0.015	Ceramic industries, coal-based industries, electronic waste, battery manufacturing, metallurgical operations, pesticides, and petroleum industries	Central nervous system damage, mental retardation, growth retardation, high blood pressure, nerve, kidney, and abdominal problem, anemia, hematopoiesis, carcinogenic, joint and muscle pain	(Gautam et al. 2016; Mubarak et al. 2016; Uddin 2017; Afroze and Sen 2018; Fu et al. 2021; Şenol and Şimşek 2022)
Arsenic	0.010	Dyes, wood preservatives, industrial dust, automobile exhaust, thermal power plants, smelting operations, mining, agriculture, and natural processes	Gastrointestinal problems, liver tumors, carcinogenic, diabetes, skin disease, depression, encephalopathy, polyneuropathy, melanosis, hepatomegaly, hemolysis, nervous system, and cardiovascular disturbances	(Beralus et al. 2014; Gautam et al. 2016; Uddin 2017; Afroze and Sen 2018; Zawierucha et al. 2022; Guisela et al. 2022)
Vanadium	–	Natural processes (volcanic eruptions), nuclear reactors, steel manufacturing, ceramic, glass, textile, metallurgical, fertilizer, pesticide, and chemical industries	Respiratory disorders, carcinogenic, liver problems, heart diseases, kidney damage, digestive problems, and nervous system damage	(Peng et al. 2020; Wołowicz et al. 2022; Bahr et al. 2022; Kończyk et al. 2022)
Cadmium	0.005	Plastic and polyvinyl industries, galvanized pipes, pesticides, paint and pigments, petroleum industry, fuel combustion, electronic waste, battery wastes, and zinc smelting	Testicular degeneration, dyspnea, lung fibrosis, carcinogenic, weight loss, hypertension, bone lesions, renal disturbances, enzyme inhibition issues	(Chen et al. 2015; Gautam et al. 2016; Uddin 2017; Afroze and Sen 2018; Fu et al. 2021; Pang et al. 2022)
Nickel	0.100	Battery industries, thermal power plants, smelting, metallurgical operations, electroplating industries, phosphate fertilizers, paint manufacturing, and galvanization	Intestinal cancer, lung cancer, chronic bronchitis, and nasal sinus, retards lung function, skin irritations	(Dawodu and Akpomie 2014; Gautam et al. 2016; Uddin 2017; Afroze and Sen 2018; Charazińska et al. 2022; Sosun et al. 2022)
Thorium	1.5×10^{-8}	Catalyst manufacturing, sensors, refractories, solid electrolytes, laboratory activities, nuclear power plants, mining, petroleum industries, and natural processes	Irreversible damage to lungs and liver, induced carcinogenesis, death, and bone cancer	(Kaynar et al. 2015; Aziman et al. 2021; Hassan et al. 2022; Akl 2022)
Zinc	5.000	Animal manure, electroplating, smelting operations, detergents, phosphate fertilizers, battery industries, ointments and wood preservatives, dye, paint, and rubber industries	Metal-fume fever, anemia, respiratory disorders, skin irritations, stomach cramps, nausea, vomiting, restlessness, and diarrhea	(Wang et al. 2015; Gautam et al. 2016; Uddin 2017; Afroze and Sen 2018; Mudasir et al. 2020)

Table 1 (continued)

Element	USEPA (mg/L)	Source	Harmful effect	References
Mercury	0.002	Paints and adhesives, ointments, leather tanning, wood preservatives, automobile manufacturing, oil refinery, electric bulb, thermal power plants, and Chlor-alkali industries	Loss of appetite, teeth problems, gum inflammation, paralysis, diarrhea, abdominal discomfort, headache, central nervous system damage, neurotoxic effects, enzymatic problems, and genetic disorders	(Gautam et al. 2016; Uddin 2017; Afroze and Sen 2018; Mudasir et al. 2020; Tene et al. 2022)
Manganese	0.050	Glass industries, porcelain, fireworks, matches, battery cells manufacturing, and mining operations	Blindness, muscle problems, fatigue, fertility issues, fever, and growth retardation	(Dawodu and Akpomie 2014; Uddin 2017; Tran et al. 2018; Dutta et al. 2021)
Cobalt	0.100	Cobalt alloy manufacturing, fertilizer industries, sewage sludge, and natural processes (volcanoes and weathering of rocks)	Weight and hair loss, thyroid and heart problems, vision problems, nausea, vomiting, pneumonia, low blood pressure, bone defects, and lung problems	(Uddin 2017; Ranaweera et al. 2020; Maleki et al. 2021; Altunkaynak et al. 2022)

photocatalysis, precipitation, and coagulation/flocculation are just a few of the processes available (Ibeji et al. 2020; Qasem et al. 2021; Karimi et al. 2022; Xu et al. 2022b). Most of these systems, however, cannot be deployed on a large scale because of high capital costs, hazardous intermediate production, and the inability to regenerate and self-clean (Crini and Lichtfouse 2019; Ghamry and Abdelmonem 2022). Adsorption, on the other hand, is an efficient and cost-effective method for removing heavy metals and radionuclides from water at very low concentrations due to the low risk of secondary contamination, cheap cost, simplicity, ease of operation, and simple adsorbent regeneration (Lee and Shin 2021; Liu et al. 2022; Xu et al. 2022a; Ankrah et al. 2022). As a result, adsorbents like agricultural waste, biochar, activated carbon, clay, polymer, nanoparticles, metal–organic framework, graphene, chitosan, and zeolite have been used to treat heavy metal and radionuclide-contaminated water (Yu et al. 2015; Renu et al. 2017; Gupta et al. 2021; Xu et al. 2022b).

Nanomaterials have recently acquired popularity as potential adsorbents for pollutant removal in wastewater treatment. This is because nanostructured adsorbents have substantially greater efficiencies and faster adsorption rates in water treatment than traditional materials, owing to their high surface area (Sadegh et al. 2017; Tee et al. 2022). Zinc oxide nanoparticles (ZnONPs) in particular have attracted a lot of attention among nanoparticle adsorbents because of their biocompatibility, affordable price, long-term stability, surface characteristics, photocatalytic activity, nontoxicity, and powerful antibacterial activity against microbes often found in water (Akbar et al. 2019; Gu et al. 2020; Akpomie et al. 2021). As a result, various studies on the adsorption of heavy metals and radionuclides onto ZnONPs have been conducted (Kumar et al. 2013; Kaynar et al. 2014; Azizi et al. 2017; Lagashetty et al. 2020; Gu et al. 2020; Alqahtany and Khalil 2021; Davarnejad and Nikandam 2022). Due to the importance of ZnONPs in water treatment, a review of their capability as a water decontaminating agent via adsorption and photocatalysis was written (Bharti et al. 2022). Another review recorded the synthetic parameters influencing the characteristics of ZnONPs and their use in wastewater treatment (Shaba et al. 2021). Likewise, the synthesis and characterization of ZnONPs were also documented (Agarwal et al. 2017; Rl et al. 2019). However, the existing reviews lacked information on the isotherms, kinetics, and thermodynamics of adsorption onto ZnONPs, which is essential for a thorough knowledge of any adsorption process. Only a basic sectional description of heavy metal polluted water treatment was provided in the reviews. This review addresses this shortcoming by offering valuable insight into these model interpretations as they pertain to heavy metal and radioactive adsorption onto ZnO nanoparticles. The equilibrium adsorption capacities obtained for the adsorption of heavy metals

and radionuclides under different experimental conditions were examined. The isotherms, kinetics and thermodynamics were evaluated in addition to the regeneration and reuse of ZnONPs. Moreover, the mechanism of adsorption of the heavy metals and radionuclides onto ZnONPs was also considered.

Adsorption capacity of ZnONPs

The adsorption of heavy metals and radionuclides on ZnONPs can be expressed in terms of the adsorption capacity. Unlike the percentage removal, which is a representation of the adsorbate (heavy metals and radionuclides) removed from the solution, the adsorption capacity is a characteristic of the adsorbent (ZnONPs). The percentage removal only expresses the amount of adsorbate removed from the solution at equilibrium but does not give an adequate representation of the amount of adsorbate present on the adsorbent (Gu et al. 2020; Rezaei-Aghdam et al. 2021). Thus, the affinity of an adsorbent for different adsorbates is effectively compared by considering the adsorption capacity of the adsorbent for the pollutants in solution. Moreover, certain experimental factors such as solution pH, contact time, adsorbent dose, temperature, and adsorbate concentration could influence the adsorption capacity of an adsorbent material (Hegazy et al. 2021; Yadav and Dasgupta 2022). Therefore, such experimental conditions must also be provided alongside the adsorption capacity for a holistic and reliable comparison. Several studies on the adsorption of heavy metals and radionuclides onto ZnONPs presented a wide range of adsorption capacities for the various pollutants. For example, in 2015, the adsorption of thorium (IV) onto ZnONPs was performed and a high adsorption capacity of 1500 mg/g was obtained, which indicated the potency of ZnONPs for the decontamination of thorium-contaminated water (Kaynar et al. 2015). In 2017, the green synthesis of ZnONPs using zerumbone was conducted and applied for the adsorption of lead (II) ions as shown in Fig. 1. The zerumbone-mediated green synthesized ZnONPs were found to be efficient in the uptake of Pb(II) with an adsorption capacity of 15.65 mg/g at 300 K and pH 5.0 (Azizi et al. 2017). The following year, a much higher adsorption capacity of 434.8 mg/g was obtained for commercially ZnONPs for Pb(II) ions at pH 6.5 and a temperature of 298 K (Yin et al. 2018). This indicates that the method of preparation or source of the nanoparticle as well as the experimental conditions could significantly influence the adsorption capacity for a particular pollutant. In another report, solvothermal synthesized ZnONPs exhibited adsorption capacities of 5.084 mg/g, 2.248 mg,/g, and 1.761 mg/g for Cu(II), Cd(II) and Ni(II) ions, respectively, after appropriate conversions from mmol/g (Wang et al. 2018). The enhanced adsorption ability of ZnONPs toward Cu(II) revealed a relatively stronger selective adsorption. The binding force between heavy metal ions and ZnONPs accounts for such selectivity. The adsorption of heavy metal ions is

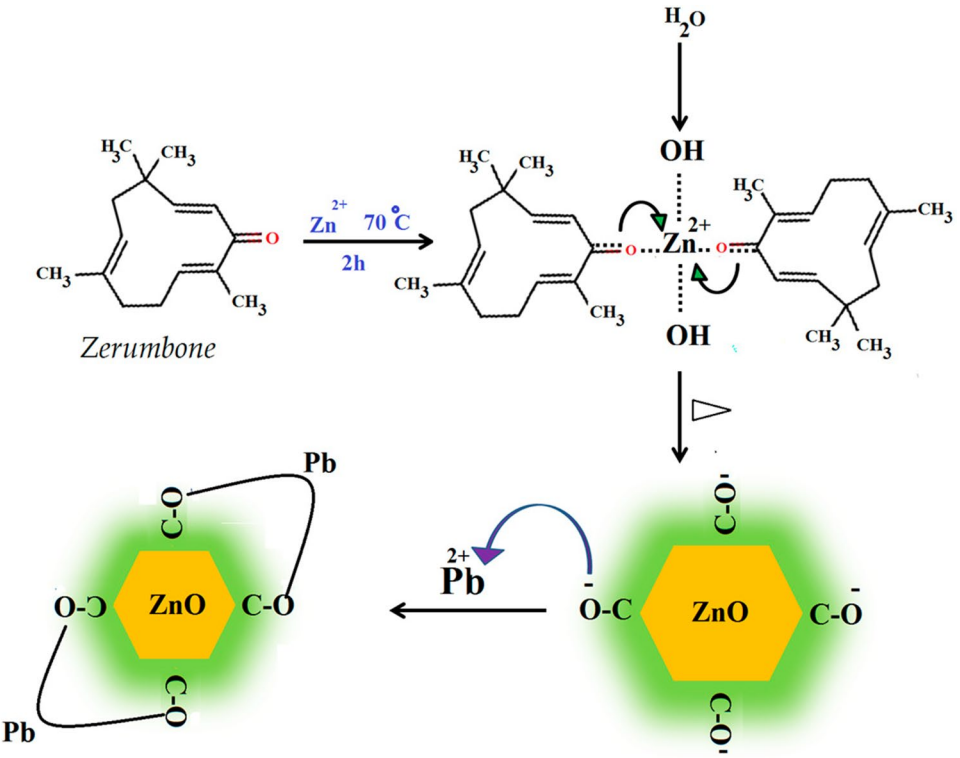

Fig. 1 The schematic representation of the green synthesis of zinc oxide nanoparticles using zerumbone and its application in the adsorption of Pb(II) ions from solution (Azizi et al. 2017). Zerumbone crystals were dissolved in 100 mL ethanol at room temperature with gentle stirring. After complete dissolution, 2.19 g of zinc acetate dihydrate was added to the zerumbone solution to react for 2 h at 70 °C with constant magnetic stirring. The white solid was recovered by centrifugation at 8000 rpm for 15 min, washed with ethanol to remove excess zerumbone, and dried for 2 h at 100 °C. The obtained ZnONPs were used for Pb(II) ions adsorption and showed the occurrence of a chelating mechanism via the zerumbone moiety

based on the electronegativity of the metal ions and the surface hydroxyl groups of ZnONPs (Wang et al. 2013). Cu(II), Ni(II), and Cd(II) have electronegativities of 2.00, 1.91, and 1.69, respectively, resulting in the strongest copper-OH bond among these three heavy metals (Wang et al. 2018). The hydrolyzable characteristics of heavy metals also alter the affinity between the heavy metals and the surface of ZnONPs. Metal ions that are easily hydrolyzed have a strong affinity for the surface (Mustafa et al. 2002). The obtained adsorption capacities followed the order Cu(II) > Ni(II) > Cd(II), which corresponds to the electronegativity order. The induced selectivity of the hydroxyl group of ZnONPs for the metal ions was verified by the attenuated total reflection-Fourier transform infrared (ATR-FTIR) before and after adsorption as shown in Fig. 2. The ATR-FTIR hydroxyl shifts at 3400 cm^{-1} and the increased metal–oxygen absorptions supported the higher uptake of Cu(II) ions onto ZnONPs. Recently, hydrothermal synthesized ZnONPs were prepared and characterized with the X-ray diffraction (XRD) as shown in Fig. 3. The hydrothermal synthesized ZnONPs revealed crystalline phases corresponding to the wurtzite hexagonal form of ZnONPs with an adsorption capacity of 64.6 mg/g for Ba(II) ions (Abdulkhair et al. 2021). The result showed

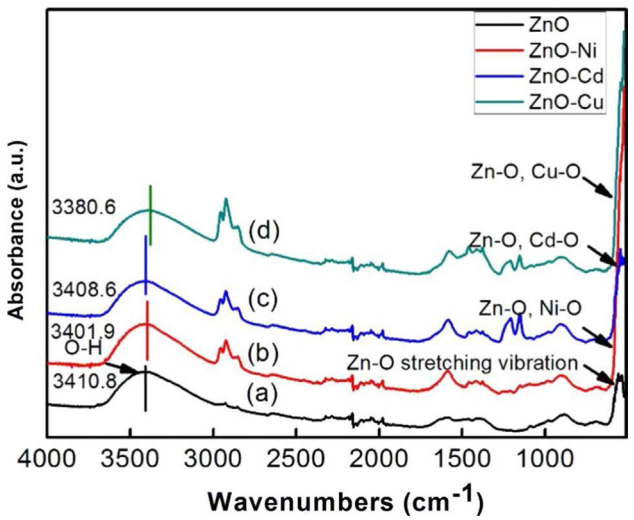

Fig. 2 The attenuated total reflection-Fourier transform infrared spectra of **a** ZnONPs before adsorption and after adsorption of **b** Ni(II) **c** Cd(II) and **d** Cu(II) ions from solution. Reproduced from (Wang et al. 2018) with permission from Elsevier. The peaks of hydroxyl groups (3400 cm^{-1}) migrated to lower wavenumbers after the adsorption of Ni, Cd, and Cu ions, showing that the adsorption might be attributed to the interaction between the metal ions and hydroxyl groups. Meanwhile, when compared to pure ZnONPs, the absorption peaks of metal-O located around 546 cm^{-1} of the Zn–O stretching enhanced after adsorption, suggesting that metal-O bonding was created after engaging with hydroxyl groups, particularly significant for the Cu–O bond. The hydroxyl group shift of ZnO (30.2 cm^{-1}) following Cu ion adsorption is larger than that of Ni (8.9 cm^{-1}) and Cd (2.2 cm^{-1}), indicating that ZnO and Cu have the strongest binding contact

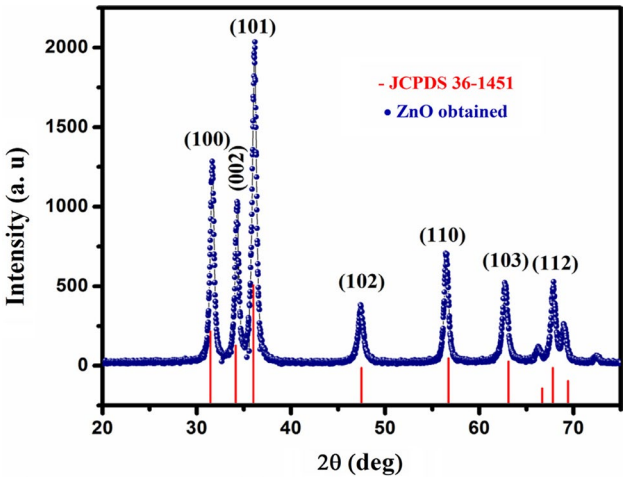

Fig. 3 The X-ray diffraction of ZnO nanoparticles prepared by hydrothermal synthesis. Reproduced from (Abdulkhair et al. 2021) with permission from Elsevier. The peaks at 31.71°, 34.38°, 36.30°, 47.52°, 56.56°, 62.91°, and 67.93° correspond to the (10 0), (0 02), (101), (102), (110), (103), and (112) planes of zinc oxide nanoparticles, respectively. The diffractions are consistent with the wurtzite hexagonal structure of zinc oxide nanoparticles (JCPDS 36-1451)

the potency of ZnONPs in the treatment of barium-polluted water via adsorption technique.

A summary of the adsorption capacity of ZnONPs for heavy metals and radionuclides uptake from solution is presented in Table 2. It is observed that the ZnONPs used so far in the adsorption of heavy metals and radionuclides apart from the commercial ones are prepared by the green, sol–gel, precipitation, solvothermal, co-precipitation, chemical reduction, hydrothermal, and the combustion methods. Moreover, the surface areas presented by the ZnONPs were in the range of 3.93–58.0 m^2/g, with the highest value obtained from the hydrothermal synthesis. The surface area was much lower than other potent adsorbents with high surface areas such as activated carbon (200–2640 m^2/g) (Pui et al. 2019) and metal–organic frameworks (1000–10,000 m^2/g)(Li et al. 2019). Despite the comparably low surface area presented by the ZnONPs, they exhibited significantly high adsorption capacities of 380–1500 mg/g for Pb(II), Cd(II), Hg(II), V(V), Th(IV), and U(VI) ions. This indicates that a low surface area of an adsorbent does not imply a low adsorption capacity of the material (Akpomie and Conradie 2020a) and that the adsorption efficiency of an adsorbent is not solely dependent on the surface area. This deduction was corroborated by the high adsorption capacity of 1111 mg/g obtained in the adsorption of U(VI) onto ZnONPs with low surface areas of 3.93–8.72 m^2/g (Kaynar et al. 2014). In general, the adsorption capacities in the range of 0.30–1500 mg/g were obtained for the adsorption of heavy metals and radionuclides onto ZnONPs except for

Table 2 Adsorption of heavy metals and radionuclides onto zinc oxide nanoparticles

Pollutant	ZnONPs preparation method	qe (mg/g)	Method of q_e determination	SA (m^2/g)	Time (min)	pH	Temp (K)	Conc (mg/L)	References
Lead(II)	Green synthesis	15.65	Langmuir	–	60	5.0	303	10	(Azizi et al. 2017)
Lead(II)	Commercial	434.8	Langmuir	–	30	6.5	298	50	(Yin et al. 2018)
Lead(II)	Sol–gel	27.4	Experimental	48.8	–	–	328	–	(Abbasi-Chianeh et al. 2019)
Lead(II)	Microwave-assisted green synthesis	595.6	Experimental	11.44	30	5.6	298	500	(Alharthi et al. 2021)
Lead(II)	Microwave-assisted green synthesis	–	–	–	60	–	–	300	(Lagashetty et al. 2020)
Lead(II)	Microwave-assisted biogenic synthesis	166.7	Langmuir	-	–	5.5	Room temp	100–200	(Radhakrishnan et al. 2016)
Lead(II)	Commercial	112.7	Experimental	31.2	120–180	6.0	298	10–300	(Mahdavi et al. 2012)
Cadmium(II)	Co-precipitation	–	–	–	120	10	–	–	(Bharti et al. 2021)
Cadmium(II)	Solvothermal	2.248	Experimental	–	600	6.0	Room temp	0.19 mmol/L	(Wang et al. 2018)
Cadmium(II)	Modified Sol–gel	217.4	Langmuir	8.25	120	7.0	328	50	(Khezami et al. 2017a)
Cadmium(II)	Microwave-assisted biogenic synthesis	149.6	Langmuir	–	–	5.5	Room temp	100–200	(Radhakrishnan et al. 2016)
Cadmium(II)	Commercial	119.1	Experimental	31.2	120–180	6.0	298	10–300	(Mahdavi et al. 2012)
Cadmium(II)	Precipitation	384	Langmuir	–	120	5.5	303	100	(Sheela et al. 2012)
Mercury(II)	Precipitation	714	Langmuir	–	120	5.5	303	100	(Sheela et al. 2012)
Mercury(II)	Microwave-assisted green synthesis	–	–	–	60	–	–	300	(Lagashetty et al. 2020)
Cobalt(II)	Sol–gel	102.1	Langmuir	8.25	720	7.0	300	50	(Khezami et al. 2017b)
Arsenic	Co-precipitation	–	–	–	15	2.0	–	–	(Bharti et al. 2021)
Arsenic(V)	Sol–gel method	1.903	Experimental	–	120	–	–	20	(Hassan et al. 2019)
Arsenic(V)	Commercial	0.85	Experimental	–	15	6.0	–	2.0	(Muensri and Danwittayakul 2017)
Arsenic(III)	Precipitation	52.63	Langmuir	–	105	7.0	323	30–90	(Yuvaraja et al. 2018)
Palladium(II)	Green synthesis	83.33	Langmuir	–	91	55	Ambient temp	77.5	(Davarnejad and Nikandam 2022)
Copper(II)	Commercial	− 18.28	Langmuir	45.58	1200	4.8	Room temp	25	(Leiva et al. 2021)
Copper(II)	Commercial	91.74	Langmuir	–	30	6.0	298	20–100	(Ali and Hassan 2022)

Table 2 (continued)

Pollutant	ZnONPs preparation method	qe (mg/g)	Method of q_e determination	SA (m^2/g)	Time (min)	pH	Temp (K)	Conc (mg/L)	References
Copper(II)	Green synthesis and gelatinization	10.95–20.43	Langmuir	–	240	4.0	298	50	(Primo et al. 2020)
Copper(II)	Solvothermal	5.084	Experimental	–	600	6.0	Room temp	*0.19 mmol/L	(Wang et al. 2018)
Copper(II)	Commercial	137.5	Experimental	31.2	120–180	6.0	298	10–300	(Mahdavi et al. 2012)
Nickel(II)	Commercial	100	Langmuir	–	30	6.0	298	20–100	(Ali and Hassan 2022)
Nickel(II)	Solvothermal	1.761	Experimental	–	600	6.0	Room temp	*0.19 mmol/L	(Wang et al. 2018)
Nickel(II)	Commercial	48.6	Experimental	31.2	120–180	6.0	298	10–300	(Mahdavi et al. 2012)
Chromium(VI)	Precipitation	9.38	Langmuir	15.75	35	2.0	303–323	3.0	(Kumar et al. 2013)
Chromium(VI)	Surfactant-mediated chemical synthesis	12.2	Langmuir	18.39	90	2.0	323	9.0	(Pandey and Tripathi 2017)
Chromium(VI)	Chemical reduction	–	–	–	60	5.0	–	100	(Mandal and Kumar 2015)
Chromium(VI)	Microwave-assisted solvothermal synthesis	0.3–5.11	Experimental	32.1	600	4.0	–	10.8	(Zhao and Qi 2012)
Chromium(III)	Hydrothermal	88.57	Langmuir	26.78	20	3.0	–	20	(Gu et al. 2020)
Barium(II)	Hydrothermal	64.6	Langmuir	58.0	55	9.0	293	40	(Abdulkhair et al. 2021)
Zinc(II)	Precipitation	357	Langmuir	–	120	5.5	303	100	(Sheela et al. 2012)
Selenium(IV)	Co-precipitation	–	–	–	120	2.0	–	–	(Bharti et al. 2021)
Selenium(IV)	Commercial	31.95	Langmuir	–	15	4.0	353	50–300	(Huang 2015)
Lanthanum(III)	Precipitation and green synthesis	92.2–113.2	Langmuir	–	1440	4.3	298	100	(Alqahtany and Khalil 2021)
Cerium(III)	Precipitation and green synthesis	40.3–69.3	Langmuir	–	1440	4.3	298	100	(Alqahtany and Khalil 2021)
Vanadium(V)	Commercial	357.14	Langmuir	–	30	6.5	298	50	(Yin et al. 2018)
Thorium(IV)	Microwave-assisted combustion	1500	Langmuir	–	60	5.0	293	50	(Kaynar et al. 2015)
Uranium(VI)	Microwave-assisted combustion	1111	Langmuir	3.93–8.72	60	5.0	303	50	(Kaynar et al. 2014)

Cu(II) adsorption reported (Leiva et al. 2021), where a negative adsorption capacity was presented. It is rare to obtain a negative adsorption capacity for an adsorbent as other researchers obtained a positive adsorption capacity (5.084–137.5 mg/g) of ZnONPs for Cu(II) ions (Mahdavi et al. 2012; Wang et al. 2018; Primo et al. 2020; Ali and Hassan 2022). Moreover, from Table 2, several studies have been conducted on the adsorption of heavy metals on ZnONPs (except for Mn(II) ions) with only a few reports on radionuclides adsorption. Therefore, future research on adsorption onto ZnONPs should focus on the treatment of water contaminated with manganese and radionuclides such as radium, ruthenium, and radon.

Adsorption isotherm modeling

An adsorption isotherm describes the equilibrium performance of adsorbents at a constant temperature. The adsorbent, adsorbate species, and other physical parameters of the solution, such as temperature, ionic strength, and pH, all influence the equilibrium isotherm (Yan et al. 2017). Adsorption isotherms are established when the adsorbent and the adsorbate come into contact at a time when the interface concentration is in dynamic balance with the adsorbate concentration in the bulk solution. Adsorption isotherms are commonly utilized in the design of commercial adsorption processes as well as material characterization. The equilibrium isotherm provides the most crucial piece of information for a comprehensive understanding of an adsorption process (Al-Ghouti and Da'ana 2020). Furthermore, adsorption isotherm models describe the mechanistic interactions between contaminants and adsorbent materials by taking into account both adsorption parameters and equilibrium data.

The Langmuir, Freundlich, Temkin, and Dubinin–Radushkevich isotherm models are the most used isotherm models applied in the adsorption of pollutants from solution onto various adsorbents. The Langmuir isotherm is based on a monolayer surface coverage with identical and equivalent definite localized sites for adsorption. There should be no steric hindrance or lateral contact between the adsorbed molecules, even on nearby sites. The Langmuir isotherm model implies that adsorption is homogeneous, with each molecule having the same constant enthalpies and sorption activation energy. The isotherm involves no adsorbate transmigration in the surface plane, and all sites should have the same affinity for the adsorbate (Gupta et al. 2021; Hamidon et al. 2022). The Langmuir model equation is written in linear form as (Umeh et al. 2021):

$$\frac{C_e}{q_e} = \frac{1}{q_L K_L} + \frac{C_e}{q_L} \tag{1}$$

The appropriateness of the Langmuir isotherm to the adsorption process is indicated by a straight line obtained from plotting C_e/q_e against C_e. On the other hand, a reversible and non-ideal adsorption process is described by the Freundlich isotherm model. The Freundlich model, unlike the Langmuir isotherm model, is not bound to monolayer formation and can be applied to multilayer adsorption. Adsorption heat and affinities do not need to be evenly distributed across the heterogeneous surface in this model. The surface heterogeneity, as well as the exponential distribution of active sites and their energies, is defined by the Freundlich isotherm model (Al-Ghouti and Da'ana 2020). The linear expression of the Freundlich isotherm model is written as (David et al. 2020):

$$\log q_e = \log K_F + \left(\frac{1}{n}\right)\log C_e \tag{2}$$

A straight line obtained from the plot of log q_e versus log C_e confirms the applicability of the Freundlich isotherm. Furthermore, by neglecting extremely low and high concentrations, the Temkin model assumes that the heat of adsorption of all molecules in the adsorbent layer decreases linearly rather than logarithmically with coverage. It is characterized by a uniform distribution of binding energies until maximum binding energy. The Temkin equation is good for forecasting gas-phase equilibrium, but it rarely fits complex adsorption systems involving liquid-phase adsorption (Foo and Hameed 2010). The Temkin isotherm equation is written in its linearized form as:

$$q_e = B\ln A + B\ln C_e \tag{3}$$

A straight line formed by plotting q_e versus ln C_e indicates the Temkin isotherm's suitability for the adsorption process. Moreover, the Dubinin–Radushkevich isotherm model does not presuppose a homogeneous surface or a constant adsorption potential of the Langmuir model. The distribution of Gaussian energy onto heterogeneous surfaces is generally connected to this adsorption isotherm. This model, unlike the Langmuir and Freundlich isotherms, is a semiempirical equation using the pore-filling mechanism. Multilayer adsorption with Van der Waal's forces is also assumed in this model (Al-Ghouti and Da'ana 2020). The Dubinin–Radushkevich isotherm equation is written in linear form as (Dawodu and Akpomie 2014):

$$\ln q_e = \ln q_m + \beta\varepsilon^2 \tag{4}$$

Applicability of the Dubinin–Radushkevich isotherm to the adsorption is verified by a linear plot of ln q_e versus ε^2.

Table 3 shows the applied isotherm and best fit models for the adsorption of heavy metals and radionuclides onto ZnONPs. It is observed that the Freundlich. Langmuir, Temkin, Dubinin–Radushkevich, Sips, and Halsey isotherm models have been applied so far in adsorption. Moreover, the Langmuir model was found to give the best fit to the adsorption of Pb(II), Hg(II), Co(II), As(III), Cr(III), Ba(II), Zn(II), Se(IV) and V(V) with coefficients of determination (R^2) in the range 0.988–1.000. However, in one of the studies, the Sips isotherm also provided the best fit alongside the Langmuir model in the adsorption of Pb(II) ions (Radhakrishnan et al. 2016). The implication of the good fit of the Langmuir model to the adsorption of these metal ions on ZnONPs is that process is restricted to monolayer adsorption onto a homogenous surface. On the other hand, the Freundlich model presented the best fit to the radionuclide adsorption of Pd(II), La(III),and

Table 3 The isotherm modeling of heavy metals and radionuclides adsorption onto ZnO nanoparticles

Adsorbate	Isotherm models applied	Best-fitted model	Coefficient of determination (R^2)	Constants for the best-fitted model	Freundlich n value	References
Lead(II)	Langmuir, Freundlich, Temkin	Langmuir	0.9970	$K_L = 0.3898$	2.504	(Yin et al. 2018)
Lead(II)	Langmuir, Freundlich	Langmuir	0.9957	$K_L = 0.042$	20.64	(Somu and Paul 2018)
Lead(II)	Langmuir, Freundlich	Langmuir	0.988	$K_L = 0.059$	2.34	(Azizi et al. 2017)
Lead(II)	Langmuir, Freundlich, Sips	Langmuir, Sips	0.9900	$K_L = 0.19$ $Q_S = 169.23$ $K_S = 0.10$ $n_S = 1.369$	3.704	(Radhakrishnan et al. 2016)
Lead(II)	Langmuir, Freundlich	None	–	–	–	(Mahdavi et al. 2012)
Cadmium(II)	Langmuir, Freundlich	Langmuir	0.9945	$K_L = 0.026$	2.10	(Somu and Paul 2018)
Cadmium(II)	Langmuir, Freundlich	Langmuir	0.9956	$K_L = 5.2$	1.818	(Khezami et al. 2017a)
Cadmium(II)	Langmuir, Freundlich, Sips	Sips	0.9500	$Q_S = 157.2$ $K_S = 0.005$ $n_S = 0.493$	1.695	(Radhakrishnan et al. 2016)
Cadmium(II)	Langmuir, Freundlich	Freundlich	0.9920	$K_F = 3.03$	1.130	(Mahdavi et al. 2012)
Cadmium(II)	Langmuir, Freundlich	Langmuir	0.9962	$K_L = 1.814$	1.179	(Sheela et al. 2012)
Mercury(II)	Langmuir, Freundlich	Langmuir	0.9979	$K_L = 4.686$	1.676	(Sheela et al. 2012)
Cobalt(II)	Langmuir, Freundlich	Langmuir	0.9931	$K_L = 0.028$	3.31	(Somu and Paul 2018)
Cobalt(II)	Langmuir, Freundlich	Langmuir	0.9999	$K_L = 0.105$	3.00	(Khezami et al. 2017b)
Arsenic(III)	Langmuir, Freundlich	Langmuir	0.9990	$K_L = 5.42$	1.621	(Yuvaraja et al. 2018)
Palladium(II)	Langmuir, Freundlich, Temkin	Freundlich	1.000	$K_F = 5.89$	0.5	(Davarnejad and Nikandam 2022)
Copper(II)	Langmuir, Freundlich, Halsey	Halsey	0.9909	$n_H = 1.3303$	1.329	(Ali and Hassan 2022)
Copper(II)	Langmuir, Freundlich, Temkin	Freundlich	0.9880	$K_F = 264.9$	0.56	(Leiva et al. 2021)
Copper(II)	Langmuir, Freundlich	None	–	–	–	(Mahdavi et al. 2012)
Copper(II)	Langmuir, Freundlich	Langmuir	0.9920	$K_L = 0.447$	0.946	(Primo et al. 2020)
Nickel(II)	Langmuir, Freundlich, Halsey	Freundlich, Halsey	0.9942	$K_F = 4.825$ $n_H = 1.28$ $K_H = 3.768$	1.2802	(Ali and Hassan 2022)
Nickel(II)	Langmuir, Freundlich	Freundlich	0.991	$K_F = 0.319$	1.086	(Mahdavi et al. 2012)
Chromium(VI)	Langmuir, Freundlich	Langmuir, Freundlich	0.9900	$K_F = 5.37$	1.622	(Kumar et al. 2013)
Chromium(VI)	Langmuir, Freundlich	Freundlich	1.000	$K_F = 0.25$	1.0	(Pandey and Tripathi 2017)
Chromium(III)	Langmuir, Freundlich, Temkin	Langmuir	0.9951	$K_L = 0.4912$	4.167	(Gu et al. 2020)

Table 3 (continued)

Adsorbate	Isotherm models applied	Best-fitted model	Coefficient of determination (R^2)	Constants for the best-fitted model	Freundlich n value	References
Barium(II)	Langmuir, Freundlich	Langmuir	0.988	$K_L = 0.118$	4.59	(Abdulkhair et al. 2021)
Zinc(II)	Langmuir, Freundlich	Langmuir	0.9906	$K_L = 0.753$	1.354	(Sheela et al. 2012)
Selenium(IV)	Langmuir	Langmuir	> 0.9900	–	–	(Huang 2015)
Lanthanum(III)	Langmuir, Freundlich, Temkin, Dubinin–Radushkevich	Freundlich	0.983	$K_F = 0.53–1.37$	1.274–1.397	(Alqahtany and Khalil 2021)
Cerium(III)	Langmuir, Freundlich, Temkin, Dubinin–Radushkevich	Langmuir, Freundlich	0.982, 0.991	$K_L = 0.026$ $K_F = 7.26$	2.481, 2.538	(Alqahtany and Khalil 2021)
Vanadium(V)	Langmuir, Freundlich, Temkin	Langmuir	1.000	$K_L = 0.509$	4.12	(Yin et al. 2018)
Thorium(IV)	Langmuir, Freundlich, Temkin	Langmuir, Freundlich	0.9800	$K_L = 0.228$ $K_F = 11.9$	1.80	(Kaynar et al. 2015)
Uranium(VI)	Langmuir, Freundlich	Freundlich	0.9934	$K_F = 8.875$	1.22	(Kaynar et al. 2014)

U(VI) on ZnONPs attributed to a multilayer heterogeneous uptake. However, more than one isotherm model was found to be applicable in the adsorption of Cd(II), Cu(II), Ni(II), Cr(VI,) and Ce(III) indicating complex adsorption involving multiple mechanisms occurring simultaneously. Chemisorption usually includes the formation of a monolayer (Langmuir isotherm), whereas physisorption entails the formation of a multilayer (Freundlich isotherm) (Al-Ghouti and Da'ana 2020). However, it is not recommended to conclude on the chemical or physical nature of adsorption based on the good fit of the Langmuir or Freundlich model alone, rather a reliable conclusion would involve a holistic consideration of the isotherm, kinetics thermodynamics, desorption, and mechanistic interpretations. Furthermore, the favorability of the adsorption process or efficient interaction between the metal ions in solution and ZnONPs can be deduced from the Freundlich n value in the range of 1–10 (Chukwuemeka-Okorie et al. 2021). As shown in Table 3, it is observed that the values of n obtained for heavy metals and radionuclides adsorption were all in the favorable range except for a few studies involving the adsorption of Cu(II), Pb(II) and Pd(II) (Somu and Paul 2018; Primo et al. 2020; Leiva et al. 2021; Davarnejad and Nikandam 2022). This shows that metal contaminants in water and ZnONPs have a good affinity for efficient water decontamination. Besides, efficient interaction between the metal ions and ZnONPs (favorable adsorption) can also be obtained from the Langmuir separation factor ($R_L = 1/(1 + K_L C_o)$). The separation factor indicates whether the adsorption is linear ($R_L = 1$), irreversible ($R_L = 0$), unfavorable ($R_L > 1$), or favorable ($0 < R_L < 1$) (David et al. 2020). Again, the calculated R_L values (not shown) in all the studies were in the favorable range which confirms the suitability of ZnONPs in the decontamination of wastewater polluted with heavy metals and radionuclides. Other isotherms, such as Hills, Flory–Huggins, Scatchard, Redlich–Peterson, Toth, and Jovanovich models, should be included in future studies on adsorption onto ZnONPs to provide more insight into the adsorption process.

Kinetics of adsorption

Kinetic model assessments are crucial because they aid in the design of adsorption systems by assisting with retention times and reactor dimensions. They also provide crucial information on pollutant adsorption mechanisms involving diffusion and adsorption on active sites (Akpomie and Conradie 2020a). Adsorption is a complicated process that often involves a combination of surface adsorption and diffusion into the pores (Benjelloun et al. 2021). In the adsorption process, there are three basic steps. External mass transfer of the adsorbate from the bulk solution to the adsorbent's external surface comes first, followed by internal diffusion of the adsorbate to the sorption sites, and ultimately sorption. Some models assume that the rate-limiting stage in the adsorption process is sorption, whereas others assume that the rate-limiting step is diffusion. As a result of the fitting to the kinetic models, the adsorption mechanism may

be deduced (Largitte and Pasquier 2016). The pseudo-first-order, pseudo-second-order, and intraparticle diffusion equations are three kinetic models mostly applied in the adsorption of pollutants from solution onto various adsorbents. According to the pseudo-first-order or Lagergren model, the rate of adsorption site occupancy is proportional to the number of vacant sites (Blázquez et al. 2011). The pseudo-first-order equation is written in linear form as (Eze et al. 2021):

$$\log\left(q_e - q_t\right) = \log q_e - \frac{K_1}{2.303}t \tag{5}$$

A linear fit obtained from the plot of log (q_e–q_t) versus t indicates the suitability of the pseudo-first-order model. On the other hand, the pseudo-second-order model assumes that sorption site occupation is proportional to the square of the number of empty sites. The pseudo-second-order equation is written in the linear form as (Pang et al. 2022):

$$\frac{t}{q_t} = \frac{1}{K_2 {q_e}^2} + \frac{t}{q_e} \tag{6}$$

A straight line obtained from the plot of t/q_t against t confirms the applicability of the pseudo-second-order model. The pseudo-first-order and pseudo-second-order models do not provide information on the diffusion mechanism, and thus, information on the mechanism of diffusion can be obtained from the intraparticle diffusion model expressed as (Umeh et al. 2021; Mogale et al. 2022):

$$q_t = K_d t^{1/2} + C \tag{7}$$

If the plot of q_t vs $t^{1/2}$ is linear and passes through the origin ($C = 0$), intraparticle diffusion is the only rate-determining step. However, adsorption is regulated by both film and intraparticle diffusion mechanisms when C is not equal to 0. The bigger the value of C and the greater the plot's divergence from linearity, the more substantial the film diffusion (boundary layer diffusion) effect (An et al. 2022).

The kinetic models applied to the adsorption of heavy metals and radionuclides onto ZnONPs are presented in Table 4. Information on the best-fitted kinetic model, coefficient of determination (R^2), and model constants for the best-fitted model and diffusion mechanism is also presented. It is evident that the pseudo-second-order model presented the best for the adsorption of all the heavy metals and radionuclides onto ZnONPs with R^2 values in the range 0.986–1.000. Many researchers over the years have attributed the best fit of the pseudo-second-order model to the chemisorption mechanism (Liu et al. 2022). Such a conclusion based on the best fit of the pseudo-second-order model alone is not recommended as this model always presents a good fit to this kinetic adsorption data irrespective of the nature of adsorption or the rate-controlling mechanism (Simonin 2016; Akpomie et al. 2017). Rather, the pseudo-second-order model's good fit shows that the rate of adsorption is controlled by both the unoccupied active sites in the adsorbent and the concentration of metal ions in the solution. It also implies that valence forces may be involved in electron exchange and sharing between the functional groups of the adsorbent and the adsorbate species (Vishan et al. 2019). This was corroborated by the previous discussion in Fig. 2, where a potent interaction between the hydroxyl groups of ZnONPs and the metals resulted in the formation of a metal–oxygen bond (Wang et al. 2018). Moreover, the pseudo-second-order rate constant (k_2) for the adsorption of different heavy metals and radionuclides on ZnONPs was in the range of 1×10^{-5}–4.42 g/mgmin. The differences in the hydrated ionic radii of metal ions influence their rate of adsorption onto adsorbents, as metals with smaller ionic radii tend to diffuse faster resulting in a faster adsorption rate. In addition, the differences in other properties of the metals, such as electronegativity, acidity strength, and the pK_{OH} values of the metal hydroxides in solution, could also influence the rate of adsorption (Barka et al. 2013). Pertaining to the diffusion mechanism of adsorption, it is evident from Table 4 that a good number of researchers did not consider this. However, the investigations available demonstrated that both film and intraparticle diffusion play a role in the overall adsorption of heavy metals and radionuclides on ZnONPs, with varying degrees of contribution. This suggests that the adsorption of the pollutants on ZnONPs is a complex process involving several mechanisms. However, in order to arrive at a more elaborate conclusion, future research on the adsorption of heavy metals and radionuclides should also take into consideration the diffusion kinetics. Moreover, additional kinetics models, such as the Elovich, Bangham, Crank, Boyd, and film diffusion, could also be used to gain a better understanding of the kinetics of adsorption onto ZnONPs (Qiu et al. 2009; Largitte and Pasquier 2016).

Thermodynamics of adsorption

The thermodynamics of adsorption is significant because it reveals how temperature influences the adsorption process. It also gives useful information about adsorption's feasibility or spontaneity, the process's exothermic or endothermic nature, the system's disorderliness or randomness, and the physical or chemical nature of adsorption (Mogale et al. 2022). The calculation of thermodynamic parameters such as Gibbs free energy changes ($\Delta G°$), entropy changes ($\Delta S°$), and enthalpy changes ($\Delta H°$) yields this crucial thermodynamic information. The three thermodynamics parameters are calculated from the Gibbs free energy and Van't Hoff's equations expressed as (Ezekoye et al. 2020):

Table 4 The kinetic modeling of heavy metals and radionuclides adsorption onto ZnO nanoparticles

Pollutant	Kinetic models applied	Best fit model	R^2	Constants for best fit model	Diffusion model	References
Lead(II)	Pseudo-first-order, Pseudo-second-order, Intraparticle diffusion, film diffusion	Pseudo-second-order	0.986	$qe_{cal}=637.6$ $K_2=0.00025$	Both intraparticle and film diffusion	(Alharthi et al. 2021)
Lead(II)	Pseudo-first-order, Pseudo-second-order, Intraparticle diffusion	Pseudo-second-order	1.000	$qe_{cal}=227.8$ $K_2=0.0093$	Boundary layer diffusion partly involves intraparticle diffusion	(Yin et al. 2018)
Lead(II)	Pseudo-first-order, Pseudo-second-order	Pseudo-second-order	0.9970 (303 K)	$qe_{cal}=4.5$ $K_2=0.048$	–	(Azizi et al. 2017)
Lead(II)	Pseudo-first-order, Pseudo-second-order	Pseudo-second-order	0.9900	$qe_{cal}=149.61$ $K_2=0.00001$	–	(Radhakrishnan et al. 2016)
Lead(II)	Pseudo-first-order, Pseudo-second-order	Pseudo-second-order	1.000	$qe_{cal}=50$ $K_2=0.011$	–	(Mahdavi et al. 2012)
Cadmium(II)	Pseudo-first-order, Pseudo-second-order	Pseudo-second-order	0.9948	$qe_{cal}=84.32$ $K_2=0.0977$	–	(Somu and Paul 2018)
Cadmium(II)	Pseudo-second-order	Pseudo-second-order	0.9980	$qe_{cal}=0.015$ $K_2=3.69$	–	(Wang et al. 2018)
Cadmium(II)	Pseudo-first-order, Pseudo-second-order	Pseudo-second-order	0.9996	$qe_{cal}=121.95$ $K_2=0.0096$	–	(Khezami et al. 2017a)
Cadmium(II)	Pseudo-first-order, Pseudo-second-order	Pseudo-second-order	0.9900	$qe_{cal}=121.81$ $K_2=0.00001$	–	(Radhakrishnan et al. 2016)
Cadmium(II)	Pseudo-first-order, Pseudo-second-order	Pseudo-second-order	0.999	$qe_{cal}=19.23$ $K_2=0.006$	–	(Mahdavi et al. 2012)
Cadmium(II)	Pseudo-first-order, Pseudo-second-order, Intraparticle diffusion	Pseudo-second-order	0.9994	$qe_{cal}=94.38$ $K_2=0.00269$	Both film diffusion and intraparticle diffusion	(Sheela et al. 2012)
Mercury(II)	Pseudo-first-order, Pseudo-second-order	Pseudo-second-order	0.9989	$qe_{cal}=133.5$ $K_2=0.0025$	Both intraparticle and film diffusion	(Sheela et al. 2012)
Cobalt(II)	Pseudo-first-order, Pseudo-second-order	Pseudo-second-order	0.9973	$qe_{cal}=71.78$ $K_2=0.029$	–	(Somu and Paul 2018)
Cobalt(II)	Pseudo-first-order, Pseudo-second-order, Intraparticle diffusion, Boyd	Pseudo-second-order	0.9983	$qe_{cal}=78.74$ $K_2=5.62$	Both pore and film diffusion	(Khezami et al. 2017b)
Arsenic(III)	Pseudo-first-order, Pseudo-second-order, Intraparticle diffusion	Pseudo-second-order	0.9890–0.9990	$K_2=0.0058$–0.0091	Intraparticle diffusion (but not solely)	(Yuvaraja et al. 2018)
Palladium(II)	Pseudo-first-order, Pseudo-second-order	Pseudo-second-order	1.000	$qe_{cal}=11.7$ $K_2=0.58$	–	(Davarnejad and Nikandam 2022)
Copper(II)	Pseudo-first-order, Pseudo-second-order	Pseudo-second-order	0.9990	$qe_{cal}=51.28$ $K_2=0.0054$	–	(Leiva et al. 2021)

Table 4 (continued)

Pollutant	Kinetic models applied	Best fit model	R^2	Constants for best fit model	Diffusion model	References
Copper(II)	Pseudo-second-order	Pseudo-second-order	0.9970	$qe_{cal}=0.13$ $K_2=0.12$	–	(Wang et al. 2018)
Copper(II)	Pseudo-first-order, Pseudo-second-order	Pseudo-second-order	1.000	$qe_{cal}=50$ $K_2=0.011$	–	(Mahdavi et al. 2012)
Copper(II)	Pseudo-first-order, Pseudo-second-order	Pseudo-second-order	0.9991	$qe_{cal}=9.67$ $K_2=4.42$	Both film diffusion and intraparticle diffusion	(Primo et al. 2020)
Nickel(II)	Pseudo-second-order	Pseudo-second-order	0.9980	$qe_{cal}=0.028$ $K_2=1.09$	–	(Wang et al. 2018)
Nickel(II)	Pseudo-first-order, Pseudo-second-order	Pseudo-second-order	0.9980	$qe_{cal}=7.87$ $K_2=0.002$	–	(Mahdavi et al. 2012)
Chromium(VI)	Pseudo-first-order, Pseudo-second-order, Intraparticle diffusion,	Pseudo-second-order	0.9900	$qe_{cal}=1.42$ (Co = 3 mg/L)	Intraparticle diffusion but not solely	(Kumar et al. 2013)
Chromium(VI)	Pseudo-first-order, Pseudo-second-order, Intraparticle diffusion,	Pseudo-second-order	0.9980 (303 K)	$qe_{cal}=21.63$ $K_2=0.015$	Mainly boundary layer diffusion, intraparticle diffusion is not the rate-limiting step	(Pandey and Tripathi 2017)
Chromium(III)	Pseudo-first-order, Pseudo-second-order, Intraparticle diffusion,	Pseudo-second-order	1.000	$qe_{cal}=19.95$ $K_2=0.003$	Boundary layer diffusion but partly involves intraparticle diffusion	(Gu et al. 2020)
Barium(II)	Pseudo-first-order, Pseudo-second-order, Intraparticle diffusion, film diffusion	Pseudo-second-order	0.9990	$qe_{cal}=62.2$ $K_2=0.62$	Film diffusion but partly involves intraparticle diffusion	(Abdulkhair et al. 2021)
Zinc(II)	Pseudo-first-order, Pseudo-second-order, Intraparticle diffusion,	Pseudo-second-order	0.9945	$qe_{cal}=59.89$ $K_2=0.00187$	Both intraparticle and film diffusion	(Sheela et al. 2012)
Lanthanum(III)	Pseudo-first-order, Pseudo-second-order, Intraparticle diffusion, Elovich	Pseudo-second-order	0.9980–0.9990	$qe_{cal}=18.70–24.78$ $K_2=0.0011$	Both boundary layer and intraparticle diffusion	(Alqahtany and Khalil 2021)
Cerium(III)	Pseudo-first-order, Pseudo-second-order, Intraparticle diffusion, Elovich	Pseudo-second-order	0.9920–0.9970	$qe_{cal}=28.89–30.41$ $K_2=0.00018–0.00028$	Both boundary layer and intraparticle diffusion	(Alqahtany and Khalil 2021)
Vanadium(V)	Pseudo-first-order, Pseudo-second-order, Intraparticle diffusion,	Pseudo-second-order	1.000	$qe_{cal}=322.58$ $K_2=0.0034$	Boundary layer diffusion (but not solely)	(Yin et al. 2018)
Thorium(IV)	Pseudo-first-order, Pseudo-second-order, Intraparticle diffusion, Elovich	Pseudo-second-order	1.000	$qe_{cal}=11.88$ $K_2=0.42$	–	(Kaynar et al. 2015)

$$\Delta G^{\circ} = -\mathrm{RT} \ln K_c \tag{8}$$

$$\ln K_C = -\left(\frac{\Delta H^{\circ}}{\mathrm{RT}}\right) + \left(\frac{\Delta S^{\circ}}{R}\right) \tag{9}$$

A linear plot of ln K_c versus 1/T allows for the determination of ΔH° and ΔS° from the slope and intercept of the plot, respectively. Generally, negative and positive values of ΔG° correspond to a spontaneous and non-spontaneous adsorption process, respectively (Eze et al. 2021). Similarly, positive and negative values of ΔS° are ascribed to an increase and decrease in randomness at the adsorbent/adsorbate interface, respectively (Singh et al. 2022). Furthermore, positive ΔH° is indicative of endothermic adsorption, while negative ΔH° values correspond to an exothermic process. Moreover, the magnitude of ΔH° in the range of 21.0–418.4 kJ/mol or less than 21.0 kJ/mol indicates the dominance of chemisorption or physisorption in the overall adsorption process, respectively (Nanthamathee and Dechatiwongse 2021). The thermodynamic parameters obtained for the adsorption of heavy metals and radionuclides onto ZnONPs are shown in Table 5. It is evident that spontaneous adsorption of the pollutants on ZnONPs was achieved in many studies due to the negative ΔH^{o} values obtained. This suggests favorable interaction between the heavy metals and radionuclides in solution and the ZnONPs adsorbent. However, a non-spontaneous removal was obtained for the adsorption of Ba(II) at a higher concentration (100 mg/L) (Abdulkhair et al. 2021), which indicates that the higher concentration was not favorable for the adsorption. This was corroborated by the decrease in the magnitude of ΔH° from 79.22 to 17.06 kJ/mol with an increase in concentration from 10 to 100 mg/L showing a shift from stronger chemical interactions to weaker physical bonding. In addition, non-spontaneous adsorption was also obtained at a higher temperature for Cd(II), Hg(II), Zn(II), and Ba(II) in some investigations (Sheela et al. 2012; Abdulkhair et al. 2021). This indicates that higher temperature was not supportive of the adsorption process as corroborated by the negative ΔH° obtained in these studies attributed to exothermic adsorption. For the ΔS°, both increase and decrease in the randomness at the ZnONPs/metal interfaces were observed in the studies, which was strongly influenced by the exothermic or exothermic nature of the process. Moreover, the uptake of some of the metals from the solution was endothermic, while others were exothermic, suggesting the suitability of ZnONPs in the adsorption of heavy metals and radionuclides at various temperatures under tropical and temperate conditions (Akpomie and Conradie 2020a). According to the magnitude of ΔH^{o}, the adsorption of Hg(II), Zn(II), Th(IV), and U(VI) is dominated by chemical forces, while the uptake of Co(II), As(III), Cu(II) and Ni(II) corresponds to a physical adsorption process. Recall from the kinetic analysis that the pseudo-second-order equation presented the best fit for all the metal ions and radionuclides. Therefore, as stated earlier, it would be misleading to conclude that an adsorption process is a chemisorption based on the good fit of the pseudo-second-order model alone. Therefore, a holistic consideration of the isotherm, kinetic, thermodynamic, and mechanism would be beneficial to arrive at a reliable classification of a process as physisorption or chemisorption.

Reusability of ZnO nanoparticles

When considering the costs of resources, adsorbent preparation, and secondary waste management, the performance of an adsorbent in reuse trials is critical for life-cycle assessment. As a result, adsorbents' chemical and physical stability must be maintained over a long period for them to be used on a large scale (Maia et al. 2021). Besides, desorption and reusability studies can also be used to determine the nature of the adsorbent–adsorbate interaction (physical or chemical adsorption) throughout the adsorption process. The adsorbate molecules are weakly bound to the adsorbent surface (physisorption), as evidenced by desorption through a neutral pH solution or water. If the desorption was carried out using a strong solvent, very acidic or basic solution, it is reasonable to assume that adsorbate molecules occupied the adsorbent surface via an ion-exchange mechanism or chemisorption (Akpomie et al. 2015). Although, this is not conclusive (Iwuozor et al. 2022). The usage of organic acid as a desorption solvent implies that a chemisorption mechanism was involved. A successful desorption process is entirely reliant on solvents that have been carefully chosen. The solvent for the desorption process should be chosen based on the adsorption mechanism. However, over the years, researchers have used desorbing solvents at random, without considering these factors (Ahmad and Danish 2022). Furthermore, an adsorbent must not only have a high adsorption capacity and quick removal kinetics, but it must also be able to be regenerated and reused over time to be designated as efficient for commercial application. Despite the importance of the reuse of adsorbents, only a few of the publications on the adsorption of heavy metals and radionuclides on ZnONPs conducted desorption and reusability experiments as shown in Table 6. So far, hydrochloric acid, sodium hydroxide, nitric acid, methanol, water, calcium chloride, and ethyl acetate have been utilized as eluents, with hydrochloric acid solution predominating. The predominance of acid solution in the desorption of metal ions could be due to the reduced adsorption of these species at low pH values due to the increased competition or replacement with hydrogen ions on the surface of the adsorbent. It is also observed that the ZnONPs were successfully regenerated and reused from 2 to 10 adsorption–desorption cycles. Moreover, the

Table 5 Thermodynamic investigations on the adsorption of heavy metals and radionuclides onto ZnO nanoparticles

Pollutant	Temp (K)	$\Delta G°$ (kJ/mol)	$\Delta S°$ (J/molK)	$\Delta H°$ (kJ/mol)	Comments	References
Lead(II)	298	− 23.3	− 191.0	− 80.30	Spontaneous, exothermic, and a decrease in randomness at ZnONP/Pb interface	(Alharthi et al. 2021)
Lead(II)	303	− 16.19	0.70	11.13	Spontaneous, endothermic, and increase in randomness at ZnONP/Pb interface	(Azizi et al. 2017)
	323	− 18.40				
	343	− 19.91				
Cadmium(II)	298	− 0.365	32.3	9.334	Spontaneous, endothermic, and increase in randomness at ZnONP/Cd interface	(Khezami et al. 2017a)
	306	− 0.775				
	313	− 1.271				
Cadmium(II)	303	− 1.662	− 82.07	− 26.11	Spontaneous at lower temperatures, non-spontaneous at higher temperatures, exothermic, and a decrease in randomness at ZnONP/Cd interface	(Sheela et al. 2012)
	313	− 0.822				
	323	− 0.143				
	333	0.499				
	343	0.172				
Mercury(II)	303	− 2.915	− 117.5	− 38.75	Spontaneous but non-spontaneous at a higher temperature of 343 K, exothermic, and a decrease in randomness at the ZnONP/Hg interface	(Sheela et al. 2012)
	313	− 2.028				
	323	− 0.890				
	333	− 0.456				
	343	2.261				
Cobalt(II)	298	− 60.83	28.0	6.075	Spontaneous, endothermic, and increase in randomness at ZnONP/Co interface	(Somu and Paul 2018)
	303	− 537.7				
	308	− 596.8				
	313	− 652.7				
Arsenic(III)	303	− 5.741	0.062	13.75	Spontaneous, endothermic, and increase in randomness at ZnONP/As interface	(Yuvaraja et al. 2018)
	313	− 5.342				
	323	− 4.538				
Copper(II)	298	− 6.704	− 9.11	− 12.25	Spontaneous, exothermic, and a decrease in randomness at ZnONP/Cu interface	(Ali and Hassan 2022)
	308	− 6.143				
	318	− 5.999				
	328	− 6.130				
Nickel(II)	298	− 7.802	− 32.83	− 17.77	Spontaneous, exothermic, and a decrease in randomness at ZnONP/Ni interface	(Ali and Hassan 2022)
	308	− 7.91				
	318	− 7.223				
	328	− 6.899				
Chromium(VI)	303	− 7.58	0.027	− 0.831	Spontaneous, exothermic, and increase in randomness at ZnONP/Cr interface	(Kumar et al. 2013)
	313	− 7.87				
	323	− 8.14				
Chromium(VI)	303	− 20.50	270	61.83	Spontaneous, endothermic, and increase in randomness at ZnONP/Cr interface	(Pandey and Tripathi 2017)
	313	− 21.65				
	323	− 25.96				
Barium(II)	293	− 5.259	− 0.252	− 79.22	Spontaneous, exothermic, non-spontaneous at 333 K, and decrease in randomness at ZnONP/Ba interface	(Abdulkhair et al. 2021)
I0 mg/L	313	− 0.213				
	333	4.838				
Barium(II)	293	3.451	− 0.070	− 17.06	Non-spontaneous, exothermic, and decrease in randomness at ZnONP/Ba interface	(Abdulkhair et al. 2021)
100 mg/L	313	4.851				
	333	6.251				

Table 5 (continued)

Pollutant	Temp (K)	$\Delta G°$ (kJ/mol)	$\Delta S°$ (J/molK)	$\Delta H°$ (kJ/mol)	Comments	References
Zinc(II)	303	−0.475	−70.64	−22.23	Spontaneous, non-spontaneous at higher temperatures, exothermic, and decrease in randomness at ZnONP/Zn interface	(Sheela et al. 2012)
	313	−0.117				
	323	0.731				
	333	1.512				
	343	2.266				
Thorium(IV)	293	−47.52	162.2	26.4	Spontaneous, endothermic, and increase in randomness at ZnONP/Th interface	(Kaynar et al. 2015)
	303	−49.12				
	313	−50.74				
Uranium(VI)	293	−46.94	160.3	28.1	Spontaneous, endothermic, and increase in randomness at the ZnONP/U interface	(Kaynar et al. 2014)
	303	−48.54				
	313	−50.15				

regeneration performance showed that ZnONPs were efficient in the uptake of Pb(II), Cd(II), Co(II), Pd(II), Ba(II), and Se(IV) ions from the solution. This proves the viability of ZnONPs for practical applications in the treatment of wastewater contaminated with these metals. However, poor regeneration and reuse were obtained in the adsorption of Cu(II) and Cr(VI) ions probably due to the poor performance of the eluent used. Therefore, other desorbing agents should be considered to achieve efficient desorption and reuse, which should be selected based on the mechanism of adsorption. Furthermore, because there are few data on the regeneration and reuse of ZnONPs in the adsorption of heavy metals and radionuclides, more research is needed.

Mechanism of adsorption onto ZnO nanoparticle

The mechanism of adsorption of heavy metals on adsorbents is usually via electrostatic interaction, hydrophobic interaction, chelation, ion exchange, hydrogen bonding, precipitation, reduction, complexation, π-π interaction, or weak Van der Waals interaction (Singh et al. 2020; Akpomie and Conradie 2020b). The adsorption process proceeds via one or a combination of two or more of these interactions. Several factors influence the mechanism, including the pH of the solution, the textural qualities of the adsorbent, and the chemical structure of the target molecules. Although pinpointing the specific interactions at work is difficult, many researchers find the Fourier transform infrared spectroscopy to be a useful technique for investigating solute–adsorbent interactions (Qureshi et al. 2020). The process might be predicted arbitrarily based on FTIR and surface charge since the adsorption mechanism is heavily influenced by surface functional groups (Ahmad and Danish 2022). The hydroxyl, amino, and carboxyl moieties are the main functional groups that interact with metals (Rajapaksha et al. 2016). However, the functional groups of ZnONPs are mainly the hydroxyl groups, and hence, we expect a limited number of mechanisms in the removal of metals since metals do not possess adequate functionalities as organic contaminants. Most investigations on the adsorption of heavy metals and radionuclides did not consider the adsorption mechanism. The few studies available only presented a cursory interpretation of the formation of bonds between the functional groups of ZnONPs and the metals (Kumar et al. 2013; Wang et al. 2018; Yuvaraja et al. 2018). Some studies proposed the complexation mechanism between the ZnONPs and metals, which was highly influenced by the solution pH (Khezami et al. 2017a; Azizi et al. 2017; Primo et al. 2020). Yin et al. reported that the surface of ZnONPs contains hydroxyl groups due to the adsorption of water and partial dissociation of water molecules (Yin et al. 2018). The abundance of hydroxyl groups affords sites for metal adsorption. The percentage of hydroxyl groups in ZnONPs dropped with the formation of metal–oxygen bonds, according to their FTIR and XPS studies, indicating that the hydroxyl groups were complexing with V(V) and Pb(II) via a complexation mechanism (Yin et al. 2018). Another study reported that the dominant mechanism in the adsorption of Cu(II) ions onto ZnONPs was complexation and precipitation based on the pH study (Mahdavi et al. 2012). An ion-exchange mechanism was observed in another work by a drop in pH of the solution following adsorption of Cd(II) and Pb(II) due to the release of hydrogen ions (Radhakrishnan et al. 2016). Furthermore, electrostatic interaction was proposed in the adsorption of Cr(VI) as a result of the drop in the zeta potential of ZnONPs from 32.6 to 19.0 mV after adsorption at pH 4.0 due to the uptake of negatively

Table 6 The reusability of ZnO nanoparticles in the adsorption of heavy metals and radionuclides

Pollutant	Desorbing agent	Cycle	Regeneration performance	References
Lead(II)	Methanol and 0.005 M HNO_3	5	Good performance, a decrease from 90.78% to 70.95% after the 5th cycle of reuse	(Alharthi et al. 2021)
Lead(II)	0.1 N HCl	5	Good performance, adsorption capacity decreased by 10–13% after the 5th cycle of reuse	(Somu and Paul 2018)
Lead(II)	0.1 M HCl	6	Efficient performance, only a slight decrease in adsorption after the 6th cycle	(Radhakrishnan et al. 2016)
Cadmium(II)	0.1 N HCl	5	Good performance, adsorption capacity decreased by 10–13% after the 5th cycle of reuse	(Somu and Paul 2018)
Cadmium(II)	Ethylacetate, methanol, and distilled water	3	Efficient performance, decrease percentage recovery from 90 to 79% after the 3rd cycle	(Khezami et al. 2017a)
Cadmium(II)	0.1 M HCl	6	Efficient performance, no significant change in adsorption after the 6th cycle	(Radhakrishnan et al. 2016)
Cobalt(II)	0.1 N HCl	5	Good performance, adsorption capacity decreased by 10–13% after the 5th cycle of reuse	(Somu and Paul 2018)
Palladium(II)	HNO_3	10	Efficient regeneration performance, only a slight decrease in adsorption from 99.24% to 93.8% after the 10th cycle	(Davarnejad and Nikandam 2022)
Copper(II)	Acid	3	Poor performance, less than 50% of the initial uptake after the 1st cycle of reuse	(Wang et al. 2018)
Chromium(VI)	0.1 N NaOH	2	Poor performance, a significant decrease in the adsorption of Cr(VI) from 93% to 18.6% after the 2nd cycle	(Kumar et al. 2013)
Chromium(VI)	–	–	Authors claim the reusability was tested and the adsorbent was found to be promising but no result on the reusability was provided in the manuscript	(Mandal and Kumar 2015)
Barium(II)	Double-distilled water and calcination at 400 °C for 2 h	4	Efficient performance, a slight decrease from 81 to 74% after the 4th cycle	(Abdulkhair et al. 2021)
Cadmium(II), Copper(II), Nickel(II), Lead(II)	Deionized water and 0.01 M CaCl2	–	The highest desorption efficiency of 82.5% was obtained for Cd (II), but the other metals had poor desorption (< 40%). Reusability was not performed	(Mahdavi et al. 2012)
Selenium(IV)	0.5 M NaOH	5	Excellent performance, no obvious decrease in the uptake of Se (IV) after the 5th cycle of reuse	(Huang 2015)

charged chromium species (Zhao and Qi 2012). Therefore, based on these reports, the complexation, precipitation, ion exchange, and electrostatic interactions are the probable mechanisms in the adsorption of heavy metals and radionuclides on ZnONPs with a predominance of complexation. However, due to the limited and superficial data currently available, future studies should focus on and undertake an in-depth analysis of the mechanism of adsorption of heavy metals and radionuclides onto ZnONPs.

Conclusions and future recommendations

The poisoning of ambient waters with heavy metals and radionuclides is on the rise as a result of rapid technological improvement. Humans and the ecosystem are both at risk from these toxins. Adsorption onto zinc oxide nanoparticles (ZnONPs) has been proven to be an efficient and low-cost method for treating contaminated wastewater. As a result, various investigations on the adsorption of heavy metals and radionuclides onto ZnONPs have been done. In this review, we looked at the isotherm, kinetics, thermodynamics, and mechanism of adsorption of the contaminants on ZnONPs to gain a better understanding of the adsorption process. The ZnONPs produced using various techniques had surface areas ranging from 3.93 to 58.0 m^2/g and adsorption capacities ranging from 0.30 to 1500 mg/g. In the isotherm analysis, the Langmuir model was shown to be the best fit for the adsorption of Pb(II), Hg(II), Co(II), As(III), Cr(III), Ba(II), Zn(II), Se(IV), and V(V), whereas the Freundlich model was adequate for Pd(II), La(III), and U(VI). The Langmuir separation factor showed favorable adsorption onto ZnONPs in all cases. The kinetic evaluation revealed that the pseudo-second-order model presented the best fit in all reports with the occurrence of both film and intraparticle diffusion mechanisms. The pseudo-second-order rate constant (k_2) for the adsorption on ZnONPs was in the range of 1×10^{-5}–4.42 g/mgmin. Thermodynamics revealed spontaneous adsorption of the heavy metals and radionuclides on ZnONPs (not in all cases). Moreover, both endothermic and exothermic processes were observed. Desorption investigations showed that hydrochloric acid, sodium hydroxide, nitric acid, methanol, water, calcium chloride, and ethyl acetate have been utilized as eluents with the predominance of hydrochloric acid. ZnONPs exhibited potent reusability in the uptake of Pb(II), Cd(II), Co(II), Pd(II), Ba(II), and Se(IV) ions but displayed poor performance for Cu(II) and Cr(VI). The complexation, precipitation, ion exchange and electrostatic interactions were the probable mechanisms in the adsorption of heavy metals and radionuclides on ZnONPs with a predominance of complexation. The overview demonstrated the potential of ZnONPs as an efficient adsorbent in the decontamination of heavy metal and radionuclide-contaminated wastewater.

The investigations that are now available have some flaws or information gaps. Therefore, these flaws must be considered to broaden the scope of the application of ZnONPs for the adsorption of heavy metals and radionuclides. Since industrial effluents contain various metal ions and radionuclides, more research into the competitive adsorption of these pollutants from multipollutant systems is needed. There are currently no studies on the adsorption of manganese and radionuclides such as radium, ruthenium and radon onto ZnONPs, these aspects should also be considered. In the isotherm analysis, only the Langmuir, Freundlich, Temkin, Dubinin–Radushkevich, Halsey and Sips isotherms have been analyzed. Therefore, other isotherms, such as Hills, Flory–Huggins, Scatchard, Redlich–Peterson, Toth and Jovanovich models, should be incorporated to gain a better understanding of the adsorption process. Few studies evaluated the diffusion mechanism of adsorption; therefore, future research should also consider this. Moreover, additional kinetics models such as Bangham, Crank, Boyd and film diffusion could be applied to gain a better understanding of the kinetics of adsorption onto ZnONPs. Future investigations should consider holistically the isotherm, kinetic, thermodynamic and mechanism of adsorption when determining whether a process is a chemisorption or physisorption. This is to prevent drawing erroneous conclusions about a chemisorption mechanism based solely on the good fit of the pseudo-second-order model. The reusability of ZnONPs in the adsorption of heavy metals and radionuclides is currently limited in the investigation. Future research should take this into account by using highly efficient solvents, selected based on the adsorption mechanism to obtain optimum reusability. There are currently no comprehensive investigations on the mechanism of metal and radionuclide adsorption on ZnONPs, which should be examined to fully comprehend the treatment process. Considering these aspects will help provide significant insights into the design of ZnONPs adsorption systems for the treatment of real wastewater polluted with heavy metals and radionuclides.

Funding Dr. Kovo Akpomie is grateful to the National Research Foundation (NRF) South Africa for the grant (Grant No. 145407) and the Central Research Fund of the University of the Free State for the postdoctoral support.

Data availability Not applicable.

Declarations

Conflict of interest The authors declare no conflict of interest.

Open Access This article is licensed under a Creative Commons Attribution 4.0 International License, which permits use, sharing, adaptation, distribution and reproduction in any medium or format, as long as you give appropriate credit to the original author(s) and the source, provide a link to the Creative Commons licence, and indicate if changes were made. The images or other third party material in this article are included in the article's Creative Commons licence, unless indicated otherwise in a credit line to the material. If material is not included in the article's Creative Commons licence and your intended use is not permitted by statutory regulation or exceeds the permitted use, you will need to obtain permission directly from the copyright holder. To view a copy of this licence, visit http://creativecommons.org/licenses/by/4.0/.

References

Abbasi-Chianeh V, Bostani B, Noroozi Z et al (2019) Enhanced structural, adsorption, and antibacterial properties of ZnO nanoparticles. J Aust Ceram Soc 55:639–644. https://doi.org/10.1007/s41779-018-0273-5

Abdulkhair B, Salih M, Modwi A et al (2021) Adsorption behavior of barium ions onto ZnO surfaces: experiments associated with DFT calculations. J Mol Struct 1223:128991. https://doi.org/10.1016/j.molstruc.2020.128991

Afroze S, Sen TK (2018) A review on heavy metal ions and dye adsorption from water by agricultural solid waste adsorbents. Water Air Soil Pollut 229:1–50. https://doi.org/10.1007/s11270-018-3869-z

Agarwal H, Venkat Kumar S, Rajeshkumar S (2017) A review on green synthesis of zinc oxide nanoparticles–an eco-friendly approach. Resour Technol 3:406–413. https://doi.org/10.1016/j.reffit.2017.03.002

Ahmad T, Danish M (2018) Prospects of banana waste utilization in wastewater treatment: a review. J Environ Manag 206:330–348. https://doi.org/10.1016/j.jenvman.2017.10.061

Ahmad T, Danish M (2022) A review of avocado waste-derived adsorbents: characterizations, adsorption characteristics, and surface mechanism. Chemosphere 296:134036. https://doi.org/10.1016/j.chemosphere.2022.134036

Akbar A, Sadiq MB, Ali I et al (2019) Synthesis and antimicrobial activity of zinc oxide nanoparticles against foodborne pathogens Salmonella typhimurium and Staphylococcus aureus. Biocatal Agric Biotechnol 17:36–42. https://doi.org/10.1016/j.bcab.2018.11.005

Akl ZF (2022) A comparative investigation of uranium and thorium adsorption behavior on amidoximated copolymeric hydrogel. J Radioanal Nucl Chem 331:1859–1867. https://doi.org/10.1007/s10967-022-08250-z

Akpomie KG, Conradie J (2020a) Banana peel as a biosorbent for the decontamination of water pollutants. Rev Environ Chem Lett 18:1085–1112. https://doi.org/10.1007/s10311-020-00995-x

Akpomie KG, Conradie J (2020b) Advances in application of cotton-based adsorbents for heavy metals trapping, surface modifications and future perspectives. Ecotoxicol Environ Saf 201:110825. https://doi.org/10.1016/j.ecoenv.2020.110825

Akpomie KG, Dawodu FA, Adebowale KO (2015) Mechanism on the sorption of heavy metals from binary-solution by a low cost montmorillonite and its desorption potential. Alex Eng J 54:757–767. https://doi.org/10.1016/j.aej.2015.03.025

Akpomie KG, Onoabedje EA, Alumona TN et al (2017) Attenuation of methylene blue from aqua-media on acid activated montmorillonite of Nigerian origin. J Environ Sci Manag 20:17–27

Akpomie KG, Ghosh S, Gryzenhout M, Conradie J (2021) One-pot synthesis of zinc oxide nanoparticles via chemical precipitation for bromophenol blue adsorption and the antifungal activity against filamentous fungi. Sci Rep 11:8305. https://doi.org/10.1038/s41598-021-87819-2

Al-Ghouti MA, Da'ana DA (2020) Guidelines for the use and interpretation of adsorption isotherm models: a review. J Hazard Mater 393:122383. https://doi.org/10.1016/j.jhazmat.2020.122383

Alharthi MN, Ismail I, Bellucci S, Salam MA (2021) Green synthesis of zinc oxide nanoparticles by Ziziphus jujuba leaves extract: environmental application, kinetic and thermodynamic studies. J Phys Chem Solids 158:110237. https://doi.org/10.1016/j.jpcs.2021.110237

Ali NJ, Hassan K (2022) Adsorption isotherm study of Cu(II) and Ni(II) on commercial zinc oxide nanoparticle. Egypt J Chem 65:235–242. https://doi.org/10.21608/ejchem.2021.85012.4144

Alqahtany FZ, Khalil M (2021) Adsorption of 140La and 144Ce radionuclides on ZnO nanoparticles: equilibrium and kinetics studies. J Radioanal Nucl Chem 327:91–104. https://doi.org/10.1007/s10967-020-07447-4

Altunkaynak Y, Canpolat M, Yavuz Ö (2022) Adsorption of cobalt(II) ions from aqueous solution using orange peel waste: equilibrium, kinetic and thermodynamic studies. J Iran Chem Soc 19:2437–2448. https://doi.org/10.1007/s13738-021-02458-8

Amaku JF, Ogundare SA, Akpomie KG, Conradie J (2021) Enhanced sequestration of Cr(VI) onto plant extract anchored on carbon-coated aluminium oxide composite. Environ Sci Pollut Res. https://doi.org/10.1007/s11356-021-14694-9

Amaku JF, Ogundare SA, Akpomie KG, Conradie J (2022) Pentaclethra macrophylla stem bark extract anchored on functionalized MWCNT-spent molecular sieve nanocomposite for the biosorption of hexavalent chromium. Int J Phytoremediation 24:301–310. https://doi.org/10.1080/15226514.2021.1937930

An N, Zagorščak R, Thomas HR (2022) Adsorption characteristics of rocks and soils, and their potential for mitigating the environmental impact of underground coal gasification technology: a review. J Environ Manag 305:114390. https://doi.org/10.1016/j.jenvman.2021.114390

Ankrah AF, Tokay B, Snape CE (2022) Heavy metal removal from aqueous solutions using fly-ash derived zeolite NaP1. Int J Environ Res 16:17. https://doi.org/10.1007/s41742-022-00395-9

Asiwaju-Bello YA, Olabode OF, Ogunsuyi MT (2020) Pollution potential and causative hydrogeochemical processes in unconfined aquifer systems in a typical urban setting: emphasis on recharge and discharge areas. Appl Water Sci 10:52. https://doi.org/10.1007/s13201-019-1131-5

Aziman ES, Mohd Salehuddin AHJ, Ismail AF (2021) Remediation of thorium(IV) from wastewater: current status and way forward. Sep Purif Rev 50:177–202. https://doi.org/10.1080/15422119.2019.1639519

Azizi S, Mahdavi Shahri M, Mohamad R (2017) Green synthesis of zinc oxide nanoparticles for enhanced adsorption of lead Ions from aqueous solutions: equilibrium kinetic and thermodynamic studies. Molecules 22:831. https://doi.org/10.3390/molecules22060831

Bahr C, Jekel M, Amy G (2022) Vanadium removal from drinking water by fixed-bed adsorption on granular ferric hydroxide. AWWA Water Sci 4:e1271. https://doi.org/10.1002/aws2.1271

Barka N, Abdennouri M, El Makhfouk M, Qourzal S (2013) Biosorption characteristics of cadmium and lead onto eco-friendly dried cactus (Opuntia ficus indica) cladodes. J Environ Chem Eng 1:144–149. https://doi.org/10.1016/j.jece.2013.04.008

Bello K, Sarojini BK, Narayana B et al (2018) A study on adsorption behavior of newly synthesized banana pseudo-stem derived superabsorbent hydrogels for cationic and anionic dye removal from effluents. Carbohydr Polym 181:605–615. https://doi.org/10.1016/j.carbpol.2017.11.106

Benjelloun M, Miyah Y, Akdemir Evrendilek G et al (2021) Recent advances in adsorption kinetic models: their application to dye types. Arab J Chem 14:103031. https://doi.org/10.1016/j.arabjc.2021.103031

Beralus JM, Ruiz-Rosas R, Cazorla-Amorós D, Morallón E (2014) Electroadsorption of arsenic from natural water in granular activated carbon. Front Mater 1:28. https://doi.org/10.3389/fmats.2014.00028

Bharti JJS, Kumar G et al (2021) Abatement of organic and inorganic pollutants from drinking water by using commercial and laboratory-synthesized zinc oxide nanoparticles. SN Appl Sci 3:311. https://doi.org/10.1007/s42452-021-04294-0

Bharti JJS, Kumar SS et al (2022) A review on the capability of zinc oxide and iron oxides nanomaterials, as a water decontaminating

agent: adsorption and photocatalysis. Appl Water Sci 12:46. https://doi.org/10.1007/s13201-021-01566-3
Bird GA (2012) Uranium uranium in the environment uranium in the environment : behavior and toxicity. In: Encyclopedia of sustainability science and technology. Springer New York, New York, pp 11220–11262
Blázquez G, Martín-Lara MA, Tenorio G, Calero M (2011) Batch biosorption of lead(II) from aqueous solutions by olive tree pruning waste: equilibrium, kinetics and thermodynamic study. Chem Eng J 168:170–177. https://doi.org/10.1016/j.cej.2010.12.059
Chakraborty R, Asthana A, Singh AK et al (2022) Adsorption of heavy metal ions by various low-cost adsorbents: a review. Int J Environ Anal Chem 102:342–379. https://doi.org/10.1080/03067319.2020.1722811
Charazińska S, Burszta-Adamiak E, Lochyński P (2022) Recent trends in Ni(II) sorption from aqueous solutions using natural materials. Rev Environ Sci Bio/technol 21:105–138. https://doi.org/10.1007/s11157-021-09599-5
Chen T, Zhou Z, Han R et al (2015) Adsorption of cadmium by biochar derived from municipal sewage sludge: impact factors and adsorption mechanism. Chemosphere 134:286–293. https://doi.org/10.1016/j.chemosphere.2015.04.052
Chukwuemeka-Okorie HO, Ekemezie PN, Akpomie KG, Olikagu CS (2018) Calcined corncob-kaolinite Combo as new sorbent for sequestration of toxic metal ions from polluted aqua media and desorption. Front Chem 6:1–13. https://doi.org/10.3389/fchem.2018.00273
Chukwuemeka-Okorie HO, Ekuma FK, Akpomie KG et al (2021) Adsorption of tartrazine and sunset yellow anionic dyes onto activated carbon derived from cassava sievate biomass. Appl Water Sci 11:27. https://doi.org/10.1007/s13201-021-01357-w
Crini G, Lichtfouse E (2019) Advantages and disadvantages of techniques used for wastewater treatment. Environ Chem Lett 17:145–155. https://doi.org/10.1007/s10311-018-0785-9
Davarnejad R, Nikandam K (2022) Eco-friendly technique for preparation of ZnO nanoparticles: Pd(II) ions adsorption. Chem Eng Technol 45:1114–1123. https://doi.org/10.1002/ceat.202100435
David MK, Okoro UC, Akpomie KG et al (2020) Thermal and hydrothermal alkaline modification of kaolin for the adsorptive removal of lead(II) ions from aqueous solution. SN Appl Sci 2:1–13. https://doi.org/10.1007/s42452-020-2621-7
Dawodu FA, Akpomie KG (2014) Simultaneous adsorption of Ni(II) and Mn(II) ions from aqueous solution unto a Nigerian kaolinite clay. J Mater Res Technol 3:129–141. https://doi.org/10.1016/j.jmrt.2014.03.002
de Primo JO, Bittencourt C, Acosta S et al (2020) Synthesis of zinc oxide nanoparticles by ecofriendly routes: adsorbent for copper removal from wastewater. Front Chem 8:571790. https://doi.org/10.3389/fchem.2020.571790
Dutta D, Borah JP, Puzari A (2021) Adsorption of Mn2+ from aqueous solution using manganese oxide-coated hollow polymethylmethacrylate microspheres (MHPM). Adsorpt Sci Technol 2021:1–10. https://doi.org/10.1155/2021/5597299
Edokpayi JN, Enitan AM, Mutileni N, Odiyo JO (2018) Evaluation of water quality and human risk assessment due to heavy metals in groundwater around Muledane area of Vhembe District, Limpopo Province, South Africa. Chem Cent J 12:2. https://doi.org/10.1186/s13065-017-0369-y
Eliodorio KP, Andolfatto VS, Martins MRG et al (2017) Treatment of chromium effluent by adsorption on chitosan activated with ionic liquids. Cellulose 24:2559–2570. https://doi.org/10.1007/s10570-017-1264-3
Eze SI, Akpomie KG, Ezekoye OM et al (2021) Antibiotic adsorption by acid enhanced dialium guineense seed waste. Arab J Sci Eng 46:309–324. https://doi.org/10.1007/s13369-020-04771-5
Ezekoye OM, Akpomie KG, Eze SI et al (2020) Biosorptive interaction of alkaline modified Dialium guineense seed powders with ciprofloxacin in contaminated solution: central composite, kinetics, isotherm, thermodynamics, and desorption. Int J Phytoremediation 22:1028–1037. https://doi.org/10.1080/15226514.2020.1725869
Ezemonye LI, Adebayo PO, Enuneku AA et al (2019) Potential health risk consequences of heavy metal concentrations in surface water, shrimp (Macrobrachium macrobrachion) and fish (Brycinus longipinnis) from Benin River, Nigeria. Toxicol Reports 6:1–9. https://doi.org/10.1016/j.toxrep.2018.11.010
Falkenmark M (2022) Planning of Africa's land/water future: hard or soft landing? Ambio 51:9–12. https://doi.org/10.1007/s13280-021-01527-9
Foo KY, Hameed BH (2010) Insights into the modeling of adsorption isotherm systems. Chem Eng J 156:2–10. https://doi.org/10.1016/j.cej.2009.09.013
Fu C, Zhu X, Dong X et al (2021) Study of adsorption property and mechanism of lead(II) and cadmium(II) onto sulfhydryl modified attapulgite. Arab J Chem 14:102960. https://doi.org/10.1016/j.arabjc.2020.102960
Gao J, Zhang L, Liu S, Liu X (2022) Enhanced adsorption of copper ions from aqueous solution by two-step DTPA-modified magnetic cellulose hydrogel beads. Int J Biol Macromol. https://doi.org/10.1016/j.ijbiomac.2022.05.073
Gautam PK, Gautam RK, Banerjee S, et al (2016) Heavy metals in the environment: Fate, transport, toxicity and remediation technologies
Gendy EA, Oyekunle DT, Ali J et al (2021) High-performance removal of radionuclides by porous organic frameworks from the aquatic environment: a review. J Environ Radioact 238–239:106710. https://doi.org/10.1016/j.jenvrad.2021.106710
Ghamry MA, Abdelmonem IM (2022) Adsorption of 60Co and 154+152Eu Using graft copolymer of starch-polyacrylic acid-polyvinylsulfonic acid. J Polym Environ. https://doi.org/10.1007/s10924-022-02446-w
Gu M, Hao L, Wang Y et al (2020) The selective heavy metal ions adsorption of zinc oxide nanoparticles from dental wastewater. Chem Phys 534:110750. https://doi.org/10.1016/j.chemphys.2020.110750
Guisela BZ, DA Ohana N, Dalvani SD et al (2022) Adsorption of arsenic anions in water using modified lignocellulosic adsorbents. Results Eng 13:100340. https://doi.org/10.1016/j.rineng.2022.100340
Gupta A, Sharma V, Sharma K et al (2021) A review of adsorbents for heavy metal decontamination: growing approach to wastewater treatment. Materials 14:4702. https://doi.org/10.3390/ma14164702
Hamidon TS, Adnan R, Haafiz MKM, Hussin MH (2022) Cellulose-based beads for the adsorptive removal of wastewater effluents: a review. Environ Chem Lett 20:1965–2017. https://doi.org/10.1007/s10311-022-01401-4
Hassan MM, Devaraj NK, Wong WW, Mukter-Uz- Zaman ASM (2019) Zinc oxide nanoparticles for removal of arsenic from water. Int J Recent Technol Eng 8:117–122. https://doi.org/10.35940/ijrte.C1021.1083S19
Hassan SSM, Abdel Rahman EM, El-Subruiti GM et al (2022) Removal of uranium-238, thorium-232, and potassium-40 from wastewater via adsorption on multiwalled carbon nanotubes. ACS Omega 7:12342–12353. https://doi.org/10.1021/acsomega.2c00819
Hegazy I, Ali MEA, Zaghlool EH, Elsheikh R (2021) Heavy metals adsorption from contaminated water using moringa seeds/olive pomace byproducts. Appl Water Sci 11:95. https://doi.org/10.1007/s13201-021-01421-5

Huang T (2015) Speciation and pre-concentration of selenium with nano-ZnO as absorbent in environmental samples. Adsorpt Sci Technol 33:513–521. https://doi.org/10.1260/0263-6174.33.5.513

Ibeji CU, Akpomie KG, Ugwu CI et al (2020) Sequestration of Pb(II) onto phosphate modified fibrous Prunus Dulcis seed shell: kinetic, thermodynamic, isotherm, desorption and reusability. J Nat Fibers. https://doi.org/10.1080/15440478.2020.1848702

Imran U, Khan M, Jamal R et al (2020) Probabilistic risk assessment of water distribution system in Hyderabad, Pakistan reveals unacceptable health hazards and areas for rehabilitation. Ecotoxicol Environ Saf 191:110233. https://doi.org/10.1016/j.ecoenv.2020.110233

Iwuozor KO, Akpomie KG, Conradie J et al (2022) Aqueous phase adsorption of aromatic organoarsenic compounds: a review. J Water Process Eng 49:103059. https://doi.org/10.1016/j.jwpe.2022.103059

Ji B, Zhang W (2022) Adsorption of cerium(III) by zeolites synthesized from kaolinite after rare earth elements (REEs) recovery. Chemosphere 303:134941. https://doi.org/10.1016/j.chemosphere.2022.134941

Karimi F, Ayati A, Tanhaei B et al (2022) Removal of metal ions using a new magnetic chitosan nano-bio-adsorbent: a powerful approach in water treatment. Environ Res 203:111753. https://doi.org/10.1016/j.envres.2021.111753

Kaynar ÜH, Ayvacıklı M, Kaynar SÇ, Hiçsönmez Ü (2014) Removal of uranium(VI) from aqueous solutions using nanoporous ZnO prepared with microwave-assisted combustion synthesis. J Radioanal Nucl Chem 299:1469–1477. https://doi.org/10.1007/s10967-014-2919-2

Kaynar ÜH, Ayvacıklı M, Hiçsönmez Ü, Çam Kaynar S (2015) Removal of thorium(IV) ions from aqueous solution by a novel nanoporous ZnO: isotherms, kinetic and thermodynamic studies. J Environ Radioact 150:145–151. https://doi.org/10.1016/j.jenvrad.2015.08.014

Khan J, Lin S, Nizeyimana JC et al (2021) Removal of copper ions from wastewater via adsorption on modified hematite (α-Fe2O3) iron oxide coated sand. J Clean Prod 319:128687. https://doi.org/10.1016/j.jclepro.2021.128687

Khezami L, Taha KK, Amami E et al (2017a) Removal of cadmium (II) from aqueous solution by zinc oxide nanoparticles: kinetic and thermodynamic studies. Desalin Water Treat 62:346–354. https://doi.org/10.5004/dwt.2017.0196

Khezami L, Taha KK, Modwi A (2017b) Efficient removal of cobalt from aqueous solution by zinc oxide nanoparticles: kinetic and thermodynamic studies. Zeitschrift Für Naturforsch A 72:409–418. https://doi.org/10.1515/zna-2016-0477

Kiwaan HA, Atwee TM, Azab EA, El-Bindary AA (2020) Photocatalytic degradation of organic dyes in the presence of nanostructured titanium dioxide. J Mol Struct 1200:127115. https://doi.org/10.1016/j.molstruc.2019.127115

Kończyk J, Kluziak K, Kołodyńska D (2022) Adsorption of vanadium(V) ions from the aqueous solutions on different biomass-derived biochars. J Environ Manag 313:114958. https://doi.org/10.1016/j.jenvman.2022.114958

Kumar KY, Muralidhara HB, Nayaka YA et al (2013) Low-cost synthesis of metal oxide nanoparticles and their application in adsorption of commercial dye and heavy metal ion in aqueous solution. Powder Technol 246:125–136. https://doi.org/10.1016/j.powtec.2013.05.017

Kumar V, Katyal D, Nayak S (2020) Removal of heavy metals and radionuclides from water using nanomaterials: current scenario and future prospects. Environ Sci Pollut Res 27:41199–41224. https://doi.org/10.1007/s11356-020-10348-4

Lagashetty A, Ganiger SK, Preeti RK et al (2020) Microwave-assisted green synthesis, characterization and adsorption studies on metal oxide nanoparticles synthesized using Ficus Benghalensis plant leaf extracts. New J Chem 44:14095–14102. https://doi.org/10.1039/D0NJ01759K

Largitte L, Pasquier R (2016) A review of the kinetics adsorption models and their application to the adsorption of lead by an activated carbon. Chem Eng Res Des 109:495–504. https://doi.org/10.1016/j.cherd.2016.02.006

Lee H-S, Shin H-S (2021) Competitive adsorption of heavy metals onto modified biochars: comparison of biochar properties and modification methods. J Environ Manag 299:113651. https://doi.org/10.1016/j.jenvman.2021.113651

Leiva E, Tapia C, Rodríguez C (2021) Highly efficient removal of Cu(II) ions from acidic aqueous solution using ZnO nanoparticles as nano-adsorbents. Water 13:2960. https://doi.org/10.3390/w13212960

Lellis B, Fávaro-Polonio CZ, Pamphile JA, Polonio JC (2019) Effects of textile dyes on health and the environment and bioremediation potential of living organisms. Biotechnol Res Innov 3:275–290. https://doi.org/10.1016/j.biori.2019.09.001

Li J, Ye W, Chen C (2019) Removal of toxic/radioactive metal ions by metal-organic framework-based materials. pp 217–279

Liu T, Lawluvy Y, Shi Y et al (2022) Adsorption of cadmium and lead from aqueous solution using modified biochar: a review. J Environ Chem Eng 10:106502. https://doi.org/10.1016/j.jece.2021.106502

Mahdavi S, Jalali M, Afkhami A (2012) Removal of heavy metals from aqueous solutions using Fe3O4, ZnO, and CuO nanoparticles. J Nanoparticle Res 14:846. https://doi.org/10.1007/s11051-012-0846-0

Maia LC, Soares LC, Alves Gurgel LV (2021) A review on the use of lignocellulosic materials for arsenic adsorption. J Environ Manag 288:112397. https://doi.org/10.1016/j.jenvman.2021.112397

Maleki F, Gholami M, Torkaman R et al (2021) Cobalt(II) removal from aqueous solution by modified polymeric adsorbents prepared with induced-graft polymerization: batch and continuous column study with analysis of breakthrough behaviors. Environ Technol Innov 24:102054. https://doi.org/10.1016/j.eti.2021.102054

Mandal BK, Kumar K (2015) Synthesis and characterization of ZnO and Al2O3 nanoparticles and their application in the chromium remediation studies. J Indian Chem Soc 92:796–799

Mitra S, Chakraborty AJ, Tareq AM et al (2022) Impact of heavy metals on the environment and human health: novel therapeutic insights to counter the toxicity. J King Saud Univ Sci 34:101865. https://doi.org/10.1016/j.jksus.2022.101865

Mogale R, Akpomie KG, Conradie J, Langner EHG (2022) Dye adsorption of aluminium- and zirconium-based metal organic frameworks with azobenzene dicarboxylate linkers. J Environ Manag 304:114166. https://doi.org/10.1016/j.jenvman.2021.114166

Mubarak NM, Sahu JN, Abdullah EC, Jayakumar NS (2016) Rapid adsorption of toxic Pb(II) ions from aqueous solution using multiwall carbon nanotubes synthesized by microwave chemical vapor deposition technique. J Environ Sci 45:143–155. https://doi.org/10.1016/j.jes.2015.12.025

Mudasir M, Baskara RA, Suratman A et al (2020) Simultaneous adsorption of Zn(II) and Hg(II) ions on selective adsorbent of Dithizone-immobilized bentonite in the presence of Mg(II) ion. J Environ Chem Eng 8:104002. https://doi.org/10.1016/j.jece.2020.104002

Muensri P, Danwittayakul S (2017) Removal of arsenic from groundwater using nano-metal oxide adsorbents. In: Key Eng Mater 751 KEM pp. 766–772. https://doi.org/10.4028/www.scientific.net/KEM.751.766

Mustafa S, Shahida P, Naeem A et al (2002) Sorption studies of divalent metal ions on ZnO. Langmuir 18:2254–2259. https://doi.org/10.1021/la0014149

Nanthamathee C, Dechatiwongse P (2021) Kinetic and thermodynamic studies of neutral dye removal from water using zirconium metal-organic framework analogues. Mater Chem Phys 258:123924. https://doi.org/10.1016/j.matchemphys.2020.123924

Niu X, Elakneswaran Y, Islam CR et al (2022) Adsorption behaviour of simulant radionuclide cations and anions in metakaolin-based geopolymer. J Hazard Mater 429:128373. https://doi.org/10.1016/j.jhazmat.2022.128373

Ogbu I, Akpomie K, Osunkunle A, Eze S (2019) Sawdust-kaolinite composite as efficient sorbent for heavy metal ions. Bangladesh J Sci Ind Res 54:99–110. https://doi.org/10.3329/bjsir.v54i1.40736

Pandey M, Tripathi BD (2017) Synthesis, characterization and application of zinc oxide nano particles for removal of hexavalent chromium. Res Chem Intermed 43:121–140. https://doi.org/10.1007/s11164-016-2610-z

Pang Y, Zhao C, Li Y et al (2022) Cadmium adsorption performance and mechanism from aqueous solution using red mud modified with amorphous MnO2. Sci Rep 12:4424. https://doi.org/10.1038/s41598-022-08451-2

Peng H, Shang Q, Chen R et al (2020) Step-adsorption of vanadium(V) and chromium(VI) in the leaching solution with melamine. Sci Rep 10:6326. https://doi.org/10.1038/s41598-020-63359-z

Pui WK, Yusoff R, Aroua MK (2019) A review on activated carbon adsorption for volatile organic compounds (VOCs). Rev Chem Eng 35:649–668. https://doi.org/10.1515/revce-2017-0057

Qasem NAA, Mohammed RH, Lawal DU (2021) Removal of heavy metal ions from wastewater: a comprehensive and critical review. Npj Clean Water 4:36. https://doi.org/10.1038/s41545-021-00127-0

Qiu H, Lv L, Pan B et al (2009) Critical review in adsorption kinetic models. J Zhejiang Univ A 10:716–724. https://doi.org/10.1631/jzus.A0820524

Qureshi UA, Hameed BH, Ahmed MJ (2020) Adsorption of endocrine disrupting compounds and other emerging contaminants using lignocellulosic biomass-derived porous carbons: a review. J Water Process Eng 38:101380. https://doi.org/10.1016/j.jwpe.2020.101380

Radhakrishnan A, Rejani P, Shanavas Khan J, Beena B (2016) Effect of annealing on the spectral and optical characteristics of nano ZnO: evaluation of adsorption of toxic metal ions from industrial waste water. Ecotoxicol Environ Saf 133:457–465. https://doi.org/10.1016/j.ecoenv.2016.08.001

Rajapaksha AU, Chen SS, Tsang DCW et al (2016) Engineered/designer biochar for contaminant removal/immobilization from soil and water: potential and implication of biochar modification. Chemosphere 148:276–291. https://doi.org/10.1016/j.chemosphere.2016.01.043

Ranaweera KH, Godakumbura PI, Perera BA (2020) Adsorptive removal of Co(II) in aqueous solutions using clearing nut seed powder. Heliyon 6:e03684. https://doi.org/10.1016/j.heliyon.2020.e03684

Renu AM, Singh K (2017) Heavy metal removal from wastewater using various adsorbents: a review. J Water Reuse Desalin 7:387–419. https://doi.org/10.2166/wrd.2016.104

Rezaei-Aghdam E, Shamel A, Khodadadi-Moghaddam M et al (2021) Synthesis of TiO2 and ZnO Nanoparticles and CTAB-stabilized Fe3O4 nanocomposite: kinetics and thermodynamics of adsorption. Res Chem Intermed 47:1759–1774. https://doi.org/10.1007/s11164-020-04363-w

Rl M, Kv U, Naik D (2019) Synthesis and characterization of ZnO nanoparticles: a review. J Pharmacogn Phytochem 8:1095–1101

Saadat F, Zerafat MM, Foorginezhad S (2020) Adsorption of copper ions from aqueous media using montmorillonite-Al2O3 nano-adsorbent incorporated with Fe3O4 for facile separation. Korean J Chem Eng 37:2273–2286. https://doi.org/10.1007/s11814-020-0651-x

Sadegh H, Ali GAM, Gupta VK et al (2017) The role of nanomaterials as effective adsorbents and their applications in wastewater treatment. J Nanostructure Chem 7:1–14. https://doi.org/10.1007/s40097-017-0219-4

Şenol ZM, Şimşek S (2022) Insights into effective adsorption of lead ions from aqueous solutions by using Chitosan-Bentonite composite beads. J Polym Environ. https://doi.org/10.1007/s10924-022-02464-8

Shaba EY, Jacob JO, Tijani JO, Suleiman MAT (2021) A critical review of synthesis parameters affecting the properties of zinc oxide nanoparticle and its application in wastewater treatment. Appl Water Sci 11:48. https://doi.org/10.1007/s13201-021-01370-z

Sheela T, Nayaka YA, Viswanatha R et al (2012) Kinetics and thermodynamics studies on the adsorption of Zn(II), Cd(II) and Hg(II) from aqueous solution using zinc oxide nanoparticles. Powder Technol 217:163–170. https://doi.org/10.1016/j.powtec.2011.10.023

Simonin J-P (2016) On the comparison of pseudo-first order and pseudo-second order rate laws in the modeling of adsorption kinetics. Chem Eng J 300:254–263. https://doi.org/10.1016/j.cej.2016.04.079

Singh S, Kumar V, Datta S et al (2020) Current advancement and future prospect of biosorbents for bioremediation. Sci Total Environ 709:135895. https://doi.org/10.1016/j.scitotenv.2019.135895

Singh S, Gupta H, Dhiman S, Sahu NK (2022) Decontamination of cationic dye brilliant green from the aqueous media. Appl Water Sci 12:61. https://doi.org/10.1007/s13201-022-01596-5

Somu P, Paul S (2018) Casein based biogenic-synthesized zinc oxide nanoparticles simultaneously decontaminate heavy metals, dyes, and pathogenic microbes: a rational strategy for wastewater treatment. J Chem Technol Biotechnol 93:2962–2976. https://doi.org/10.1002/jctb.5655

Sosun AA, Mannan A et al (2022) Removal of of toxic metal ions (Ni2+ and Cd2+) from wastewater by using TOPO decorated iron oxide nanoparticles. Appl Water Sci 12:86. https://doi.org/10.1007/s13201-022-01588-5

Su M, Li H, Liu Z et al (2022) Highly-efficient and easy separation of γ-Fe2O3 selectively adsorbs U(VI) in waters. Environ Res 210:112917. https://doi.org/10.1016/j.envres.2022.112917

Tee GT, Gok XY, Yong WF (2022) Adsorption of pollutants in wastewater via biosorbents, nanoparticles and magnetic biosorbents: a review. Environ Res 212:113248. https://doi.org/10.1016/j.envres.2022.113248

Tene T, Arias Arias F, Guevara M et al (2022) Removal of mercury(II) from aqueous solution by partially reduced graphene oxide. Sci Rep 12:6326. https://doi.org/10.1038/s41598-022-10259-z

Tortajada C, Biswas AK (2018) Achieving universal access to clean water and sanitation in an era of water scarcity: strengthening contributions from academia. Curr Opin Environ Sustain 34:21–25. https://doi.org/10.1016/j.cosust.2018.08.001

Tran TN, Kim D-G, Ko S-O (2018) Adsorption mechanisms of Manganese(II) ions onto acid-treated activated carbon. KSCE J Civ Eng 22:3772–3782. https://doi.org/10.1007/s12205-018-1334-6

Uddin MK (2017) A review on the adsorption of heavy metals by clay minerals, with special focus on the past decade. Chem Eng J 308:438–462. https://doi.org/10.1016/j.cej.2016.09.029

Umeh TC, Nduka JK, Akpomie KG (2021) Kinetics and isotherm modeling of Pb(II) and Cd(II) sequestration from polluted water onto tropical ultisol obtained from Enugu Nigeria. Appl Water Sci 11:65. https://doi.org/10.1007/s13201-021-01402-8

Vardhan KH, Kumar PS, Panda RC (2019) A review on heavy metal pollution, toxicity and remedial measures: current trends and future perspectives. J Mol Liq 290:111197

Vishan I, Saha B, Sivaprakasam S, Kalamdhad A (2019) Evaluation of Cd(II) biosorption in aqueous solution by using lyophilized biomass of novel bacterial strain Bacillus badius AK: biosorption kinetics, thermodynamics and mechanism. Environ Technol Innov 14:100323. https://doi.org/10.1016/j.eti.2019.100323

Wang J, Zhuang S (2019) Covalent organic frameworks (COFs) for environmental applications. Coord Chem Rev 400:213046. https://doi.org/10.1016/j.ccr.2019.213046

Wang X, Cai W, Liu S et al (2013) ZnO hollow microspheres with exposed porous nanosheets surface: structurally enhanced adsorption towards heavy metal ions. Colloid Surf A Physicochem Eng Asp 422:199–205. https://doi.org/10.1016/j.colsurfa.2013.01.031

Wang J, Liu G, Li T, Zhou C (2015) Physicochemical studies toward the removal of Zn(ii) and Pb(ii) ions through adsorption on montmorillonite-supported zero-valent iron nanoparticles. RSC Adv 5:29859–29871. https://doi.org/10.1039/C5RA02108A

Wang X, Cai W, Panther JG et al (2018) Micro/nanostructured porous ZnO as a new DGT binding phase for selective measurement of Cu(II) in water. Colloid Surf A Physicochem Eng Asp 537:109–115. https://doi.org/10.1016/j.colsurfa.2017.10.008

Wołowicz A, Wawrzkiewicz M, Hubicki Z et al (2022) Enhanced removal of vanadium(V) from acidic streams using binary oxide systems of TiO2-ZrO2 and TiO2-ZnO type. Sep Purif Technol 280:119916. https://doi.org/10.1016/j.seppur.2021.119916

Wu X, Huang Q, Mao Y et al (2019) Sensors for determination of uranium: a review. TrAC Trends Anal Chem 118:89–111. https://doi.org/10.1016/j.trac.2019.04.026

Xiao-teng Z, Dong-mei J, Yi-qun X et al (2019) Adsorption of Uranium(VI) from aqueous solution by modified rice stem. J Chem 2019:1–10. https://doi.org/10.1155/2019/6409504

Xu C, Feng Y, Li H et al (2022a) Adsorption of heavy metal ions by iron tailings: behavior, mechanism, evaluation and new perspectives. J Clean Prod 344:131065. https://doi.org/10.1016/j.jclepro.2022.131065

Xu M, Cai Y, Chen G et al (2022b) Efficient selective removal of radionuclides by sorption and catalytic reduction using nanomaterials. Nanomaterials 12:1443. https://doi.org/10.3390/nano12091443

Yadav BS, Dasgupta S (2022) Effect of time, pH, and temperature on kinetics for adsorption of methyl orange dye into the modified nitrate intercalated MgAl LDH adsorbent. Inorg Chem Commun 137:109203. https://doi.org/10.1016/j.inoche.2022.109203

Yan X-F, Fan X-R, Wang Q, Shen Y (2017) An adsorption isotherm model for adsorption performance of silver-loaded activated carbon. Therm Sci 21:1645–1649. https://doi.org/10.2298/TSCI151202048Y

Yang J, Yu M, Chen W (2015) Adsorption of hexavalent chromium from aqueous solution by activated carbon prepared from longan seed: kinetics, equilibrium and thermodynamics. J Ind Eng Chem 21:414–422. https://doi.org/10.1016/j.jiec.2014.02.054

Yin X, Meng X, Zhang Y et al (2018) Removal of V(V) and Pb(II) by nanosized TiO2 and ZnO from aqueous solution. Ecotoxicol Environ Saf 164:510–519. https://doi.org/10.1016/j.ecoenv.2018.08.066

Yu S, Wang X, Tan X, Wang X (2015) Sorption of radionuclides from aqueous systems onto graphene oxide-based materials: a review. Inorg Chem Front 2:593–612. https://doi.org/10.1039/C4QI00221K

Yuvaraja G, Prasad C, Vijaya Y, Subbaiah MV (2018) Application of ZnO nanorods as an adsorbent material for the removal of As(III) from aqueous solution: kinetics, isotherms and thermodynamic studies. Int J Ind Chem 9:17–25. https://doi.org/10.1007/s40090-018-0136-5

Zawierucha I, Nowik-Zajac A, Girek T et al (2022) Arsenic(V) removal from water by resin impregnated with cyclodextrin ligand. Processes 10:253. https://doi.org/10.3390/pr10020253

Zhao X, Qi L (2012) Rapid microwave-assisted synthesis of hierarchical ZnO hollow spheres and their application in Cr(VI) removal. Nanotechnology. https://doi.org/10.1088/0957-4484/23/23/235604

Publisher's Note Springer Nature remains neutral with regard to jurisdictional claims in published maps and institutional affiliations.